Tectonophysics xxx (2014) xxx–xxx

Contents lists available at ScienceDirect

Tectonophysics

journal homepage: www.elsevier.com/locate/tecto

A revised crustal stress orientation database for Canada

Karsten Reiter [a,b,*], Oliver Heidbach [a], Douglas Schmitt [c], Kristine Haug [d], Moritz Ziegler [a,b], Inga Moeck [a,e]

[a] GFZ German Research Centre for Geosciences, Telegrafenberg, 14473 Potsdam, Germany
[b] University of Potsdam, Inst. of Earth and Environmental Science, Karl-Liebknecht-Straße 24-25, 14476 Potsdam-Golm, Germany
[c] Institute for Geophysical Research, CCIS 4-138, Dept. of Physics, University of Alberta, Edmonton, Alberta T6G 2E1, Canada
[d] Alberta Energy Regulator, Alberta Geological Survey, 402 Twin Atria Building, 4999,- 98 Avenue, Edmonton, Alberta T6B 2X3, Canada
[e] Technische Universität München, Dept. of Civil, Geo and Environmental Engineering, Arcisstraße 21, 80333 München, Germany

ARTICLE INFO

Article history:
Received 8 May 2014
Received in revised form 31 July 2014
Accepted 16 August 2014
Available online xxxx

Keywords:
Stress pattern
Tectonic stress
Canada
Alberta
Database
Circular statistics

ABSTRACT

The Canadian database on contemporary crustal stress has not been revised systematically in the past two decades. Here we present the results of our new compilation that contains 514 new data records for the orientation data of maximum compressive horizontal stress and 188 data records that were re-assessed. In total the Canadian stress database has now 1667 data records, which is an increase of about 45%. From these data, a new Canadian Stress map as well as one for the Province of Alberta is presented.

To analyse the stress pattern, we use the quasi median on the circle as a smoothing algorithm that generates a smoothed stress map of the maximum compressive horizontal stress orientation on a regular grid. The newly introduced quasi interquartile range on the circle estimates the spreading of the data and is used as a measure for the wave-length of the stress pattern. The result of the hybrid wavelength analysis confirms that long spatial wavelength stress patterns ($\geq$1000 km) exist in large areas in Canada. The observed stress pattern is transmitted through the intra-plate regions.

The results reveal that shorter spatial wave length variation of the maximum compressive horizontal stress orientation of less than 200 km, prevails particularly in south-eastern and western Canada. Regional stress sources such as density contrasts, active fault systems, crustal structures, etc. might have a significant impact in these regions. In contrast to these variations, the observed stress pattern in the Alberta Basin is very homogeneous and mainly controlled by plate boundary forces and body forces. The influence of curvature of the Rocky Mountains salient in southern Alberta is minimal. The present-day horizontal stress orientations determined herein have important implications for the production of hydrocarbons and geothermal energy in the Alberta Basin.

1. Introduction

Understanding of the in-situ stress tensor in the Earth's crust is of key importance to a number of major scientific, economic and societal issues. Knowledge of the crustal stress is key to understanding plate tectonics or earthquake cycles. Such knowledge is also crucial for drilling as crustal stresses influence well-bore stability, reservoir operation and stimulation, cap rock integrity, induced seismicity and the long-term stability of underground constructions. Consequently, knowledge of the contemporary crustal state of stress is of great importance to resource-rich nations such as Canada whose economies depend on the efficient and safe extraction of minerals and hydrocarbons and who is under pressure to do better at protection of the environment.

There are several methods used to estimate both stress orientation and magnitudes from borehole observations (e.g. Amadei and Stephansson, 1997; Ljunggren et al., 2003; Schmitt et al., 2012; Zang and Stephansson, 2010; Zoback et al., 2003). These methods include overcoring, analysis of the orientation of borehole breakouts and drilling induced tensile fractures, hydraulic fracturing (leak-off, mini-frac, micro-frac, etc.), earthquake focal mechanisms and geological indicators. The results from these methods may represent the stress state at scales of a few decimetres up to tens of kilometres (Ljunggren et al., 2003). However, obtaining the complete state of stress (i.e. the six independent components of the stress tensor) remains a challenging task. All techniques have in common the fact that they can provide at least the maximum compressive horizontal stress (S_{Hmax}) orientation, or perpendicularly to it, the minimum horizontal stress (S_{hmin}) azimuth; only a few methods deliver further components of the stress tensor. Furthermore, the vertical stress magnitude (S_V) can be estimated from the weight of the overburden and the S_{hmin} magnitude from leak-off tests or hydraulic fracturing (e.g. Haimson and Fairhurst, 1969; Hubbert and Willis, 1957; White et al., 2002). However, in particular the reliable estimation of the S_{Hmax} magnitude remains difficult as the numerous assumptions to be made impose high uncertainties.

Consequently, stress maps have primarily focussed on illustrating the S_{Hmax} azimuth. The first systematic compilation of orientation data

* Corresponding author at: GFZ German Research Centre for Geosciences, Telegrafenberg, 14473 Potsdam, Germany.
E-mail address: reiter@gfz-potsdam.de (K. Reiter).

http://dx.doi.org/10.1016/j.tecto.2014.08.006
0040-1951/

by Sbar and Sykes (1973) mapped the S_{Hmax} orientation over North America, by means of focal mechanisms, geological indicators, overcoring and hydraulic fracturing. Stress mapping accelerated significantly with the findings of Bell and Gough (1979) and Hottman et al. (1979) that the azimuth of borehole breakouts (Babcock, 1978) indicates the S_{Hmax} orientation. The acquisition of such data is relatively easily found by means of oriented calliper log data as is provided, for example, by dipmeters (e.g. Plumb and Hickman, 1985). The compilation of stress data in North America in the subsequent years by Adams (1987), Adams and Basham (1989), Adams and Bell (1991), Bell et al. (1994), Fordjor et al. (1983), Gough et al. (1983). Zoback and Zoback (1980, 1981, 1989, 1991) showed, that the pattern of S_{Hmax} orientations is frequently uniform over thousands of kilometres. These observations were used as evidence that the tectonic stress field is controlled by plate boundary forces and body forces; these are first order stress sources (Zoback, 1992). This hypothesis was studied globally by the continued compilation of stress data in the framework of the World Stress Map project (WSM) and is confirmed in first order (Richardson, 1992; Zoback, 1992; Zoback et al., 1989). Besides the first order main driving forces of plate tectonics, there are several stress perturbations of the second and third orders, which can strongly overprint the regional stress field in some areas (Heidbach et al., 2007; Zoback, 1992). Such local or regional effects can be detected only in the case of the availability of dense stress observations of sufficient quality.

In the two decades after the initial phase of the WSM project (1986–1992), data entries in the recent global database have been tripled (Heidbach et al., 2010). Despite this global increase there has not to our knowledge been a substantial systematic revision nor extension on the Canadian stress database for about two decades (Adams and Bell, 1991; Bell et al., 1994) with the exception of some additional work focussed on specific geological targets (e.g. Bachu et al., 2008; Bell and Bachu, 2003, 2004; Bell and Grasby, 2012). In the Western Canada Sedimentary Basin with more than 700,000 wells, a considerable amount of geophysical logging image and dipmeter has been collected, but most of this remains inaccessible. In principle, the extraordinary data density would allow a far more detailed study of second and third order stress deviations. A revised stress data compilation and analysis from the Alberta Basin which represents the foreland basin of Western Canadian Cordillera would allow the comparison of stress patterns in similar geologic settings as the Subalpine Molasse Basin, a foreland basin of the Alpine orogenic belt in Germany (Reinecker et al., 2010).

The first objective of this paper is to update and revise the stress map of Canada by adding all new stress orientation data to the existing data set. As much of the new data comes from the portions of the Western Canada Sedimentary Basin in Alberta, the pattern analysis will focus on the overall stress there. All 1153 data records from the WSM 2008 database release (Heidbach et al., 2010) were cross-checked and state of the art quality ranking was applied. By adding 514 data records from new publications and a data set from the Alberta Geological Survey (AGS), the number of S_{Hmax} azimuth records in the research area is increased by 45% to 1667.

The second objective of this work is the investigation of the S_{Hmax} orientation pattern in Canada and again in detail for Alberta, by means of the updated database. A hybrid wavelength analysis technique based on the algorithm from Heidbach et al. (2010) is developed further and presented here.

Furthermore, the data set showcases a more homogeneous stress pattern along the length of Alberta. In particular this new compilation appears to show that the S_{Hmax} orientations in the Alberta foreland basin are not always perpendicular to the front of the Rocky Mountains as had previously been believed (e.g. Bell and Gough, 1979). That is the first and second order patterns dominate over Alberta despite the existence of large bounding geomorphological features such as the Rocky Mountains and the Rocky Mountains Trench further to the west. This is in contrast to other regions such as the St. Lawrence Lowland where a good observation density suggests a stress field dominated by the second and third order stress sources (e.g. fault zones).

2. Crustal stresses

2.1. Indicators of stress orientation

The full stress tensor consists of six independent components none of which can be measured directly. Most of our stress knowledge comes from stress indicators that are observed by the use of a variety of methods from boreholes. These methods (for overview see Ljunggren et al., 2003) may be distinguished as they provide either data on crustal stress orientations only or they give knowledge of the stress magnitudes and/or faulting regime. Here, we will focus only on those methods which allow for estimation of the stress orientation.

Since the 19*th* century, structural geologists have interpreted and quantified rock deformations under the assumption that ancient stress conditions lead to the observed deformation pattern in the rock mass. Therefore recent crustal deformation is interpreted to be caused by the recent stress field or remnant stresses such as those induced by glacio-isostatic rebound from Pleistocene glaciations (Sbar and Sykes, 1973, and references therein). Precise dating of stress indicators helps to exclude palaeo-stress indicators. Stress- and strain markers in rock can be variable depending on rock type, deformation rate and stress regime potentially causing shear, shortening or extension. Among others geological indicators include dykes or volcanic vent alignments (GVA) (Nakamura, 1977; Nakamura et al., 1977), fault slip data (GF) (e.g. Angelier, 1979, 1984) and pop-up structures or joint systems (Hancock, 1991; Hancock and Engelder, 1989).

Bell and Gough (1979) and independently Hottman et al. (1979) were the first to recognize that borehole breakouts (BO), which were known for some years (e.g. Babcock, 1978; Cox, 1972), are an indicator of the orientation of stresses in the crust. Breakouts are borehole segments of several metres or more along which the borehole wall has spalled preferentially at diametrically opposed azimuths. As such, the diameter across the BO must be greater than that for the drill bit; and this major axis points in the direction of S_{hmin}. The breakouts occur due to concentration of the combined horizontal stresses at the borehole wall (e.g. Haimson and Song, 1993; Schmitt et al., 2012; Zoback et al., 1985, 2003). There are several geophysical logging methods to identify elliptical borehole sections that include ultrasonic acoustic imaging as produced by the borehole televiewer (Zemanek et al., 1969, 1970), electrical resistivity imaging methods such as produced by micro-resistivity tools (Ekstrom et al., 1987), and simpler mechanical oriented-calliper logs like four-arm up to multi-finger dipmeter/calliper logs (e.g. Babcock, 1978; Plumb and Hickman, 1985; Reinecker et al., 2003).

Drilling induced (tensile) fractures (DIF) also provide stress orientation data. They are also related to the superposition of the far-field

Table 1
Type and quality of the S_{Hmax} orientation data from Canada and surrounding (latitude 41°N, longitude 142°W to 46°W).

Data type	Complete dataset		New data only	
	A–E	A–C	A–E	A–C
	Quality		Quality	
Focal mechanisms (FMF, FMS, FMA)	767	516	212	132
Borehole breakouts (BO, BOT)	657	389	181	38
Drilling-induced tensile fractures (DIF)	42	38	42	38
Geological: fault–slip (GFM, GFS)	6	6		
Hydraulic fracturing (HF, HFG, HFM)	43	13	20	4
Overcoring (OC)	91	12	53	4
Geological: volcanic alignment (GVA)	53	3		
Petal centreline fractures (PC)	4	4	4	4
Shear wave splitting (SW)	4		2	
Total	1667	981	514	220

Please cite this article as: Reiter, K., et al., A revised crustal stress orientation database for Canada, Tectonophysics (2014), http://dx.doi.org/10.1016/j.tecto.2014.08.006

Table 2
First, second and third order stress sources, modified after Zoback et al. (1989), Zoback (1992), Heidbach et al. (2007, 2010).

Order of stress source	Extent vs. lithosphere thickness	Extent [km]	Stress sources
First	≫	>500	Plate boundary forces: ridge push, slab pull, trench suction; gravitational potential energy; basal tractions originating from density driven mantle convection
Second	~	100–500	Lithospheric flexure (isostatic compensation, sediment loading on continental margins, seamount loading, upwarping ocean-ward of the trench), localized lateral density contrasts/buoyancy forces, lateral strength contrasts (anisotropy of material properties), topography, continental rifting, large fault zones, lateral contrasts of heat production, erosion
Third	≪	<100	Local density or strength contrasts, basin geometry, basal detachment, man-made excavation, man-made downhole pressure changes, impoundment dams, lowering of the water table, active faults, incised valleys

tectonic stresses and the borehole fluid pressure at the borehole wall, and they result when the concentrated stresses become tensile. This occurs in the direction of the greatest horizontal compressive stress — the orientation of the DIF indicates that for S_{Hmax}. Some care must be taken in their interpretation as the fractures are sometimes misinterpreted as borehole breakouts (Barton and Moos, 2010; Brudy and Kjørholt, 2001). When carefully employed, however, the DIF are also reliable estimator of the stress orientation (Aadnøy and Bell, 1998; Tingay et al., 2008; Zoback et al., 2003).

Leak-off methods are very commonly used to test borehole integrity, and are similar to the hydraulic fracturing method (HF) (e.g. Haimson and Fairhurst, 1969; Hubbert and Willis, 1957; Schmitt et al., 2012; White et al., 2002; Zoback et al., 2003). If the pressurization records are appropriately made, they can be used to measure the magnitude of the least compressive principal stress (σ_3). This is often interpreted to be the same as the magnitude of S_{hmin}, if the tensile fracture is vertical in strike–slip and normal faulting environments. If the induced fracture can be detected by the use of borehole image logging or by deformation of a rubber packer by intrusion, its azimuth indicates the orientation of S_{Hmax}.

The overcoring (OC) method (McGarr and Gay, 1978; Obert, 1962) in general isolates a rock cylinder with a diameter of about 3 cm and a length of about 30–60 cm from the surrounding rock. The measured elastic relaxation of the rock cylinder is assumed as equivalent to the stress magnitude as well as occurring in the direction of stress orientation, before removal of the surrounding rock. The method allows the three-dimensional measurement of strain relief, but is usually only applied close to the surface. A further drawback of strain relief measurements is the costs and the small amount of measured rock mass.

Earthquakes occur, when the elastically accumulated stress overcomes the internal friction of the rocks or the external friction along

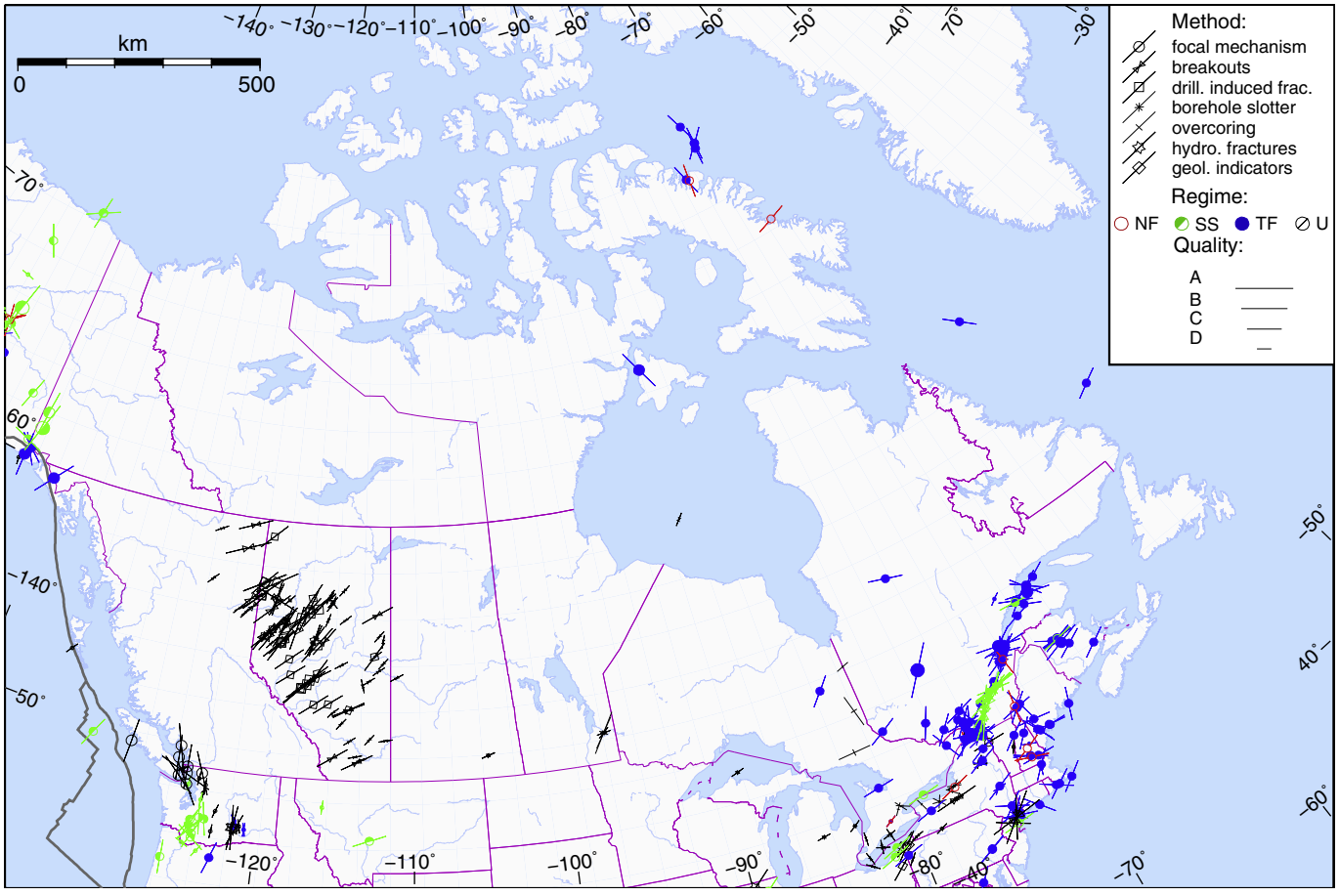

Fig. 1. New data in the Canadian database, added since the 2008 World Stress Map update (Heidbach et al., 2009, 2010). Lines represent orientations of maximum horizontal compressional stress (S_{Hmax}), line length is proportional to quality. Colours indicate stress regimes, with red for normal faulting (NF), green for strike–slip faulting (SS), blue for thrust faulting (TF), and black for unknown regime (U). Plate boundaries are taken from the global model PB2002 of Bird (2003). (For interpretation of the references to colour in this figure legend, the reader is referred to the web version of this article.)

Please cite this article as: Reiter, K., et al., A revised crustal stress orientation database for Canada, Tectonophysics (2014), http://dx.doi.org/10.1016/j.tecto.2014.08.006

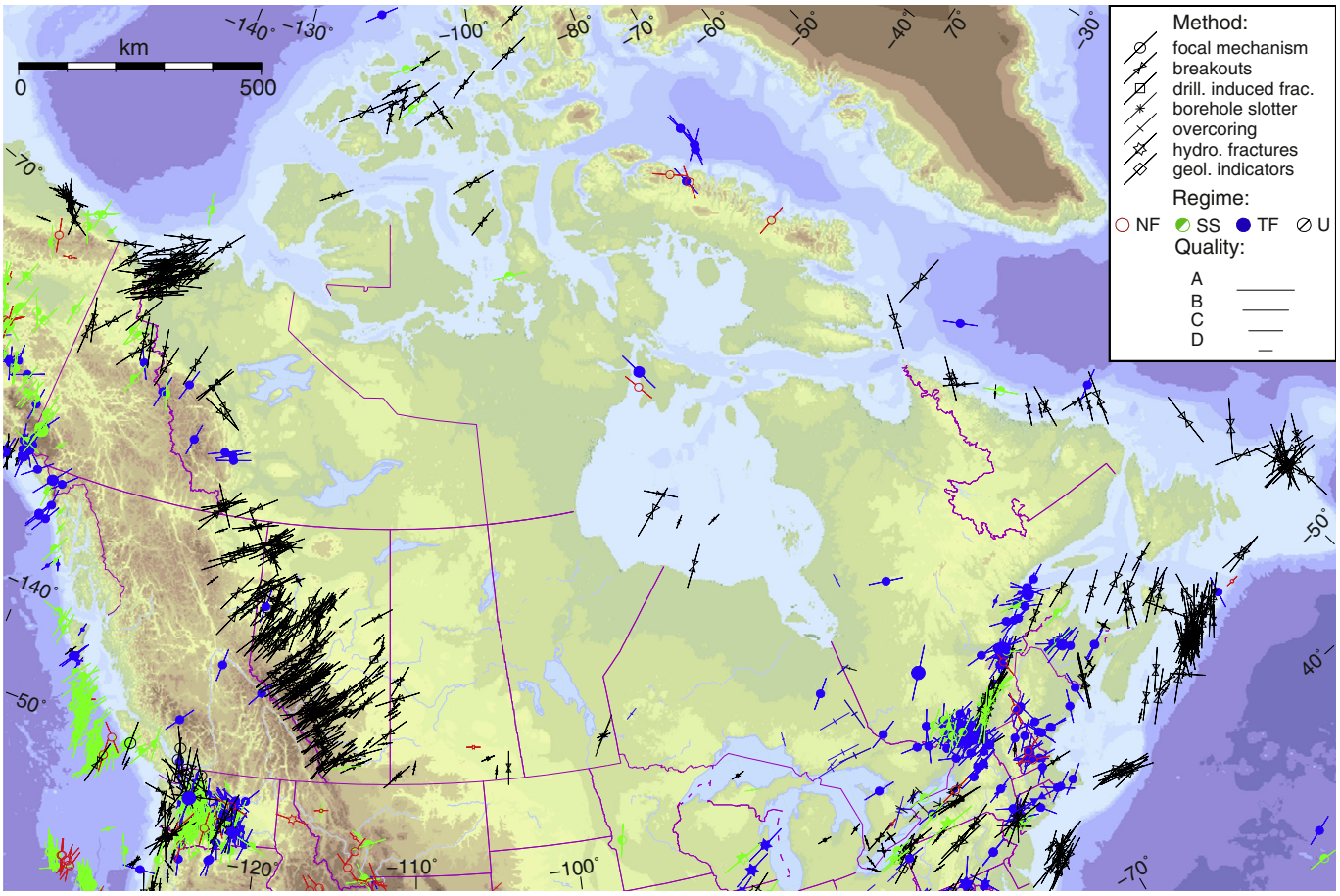

Fig. 2. Stress map of Canada including topography with the complete compiled dataset. Lines represent orientations of maximum horizontal compressional stress (S_{Hmax}), line length is proportional to the quality. Colours indicate stress regimes, with red for normal faulting (NF), green for strike–slip faulting (SS), blue for thrust faulting (TF), and black for unknown regime (U). Plate boundaries are taken from the global model PB2002 of Bird (2003). (For interpretation of the references to colour in this figure legend, the reader is referred to the web version of this article.)

existing faults. This relative motion is used on the surface as geological indicators. At remote depths, single focal mechanisms (FMS) are used as indicators for the S_{Hmax} azimuth (McKenzie, 1969; Raleigh et al., 1972). Average or composite focal mechanisms (FMA) combine several single focal mechanism solutions. Due to the characteristics of a focal mechanism solution and the P-, B-, T-axes, the derived orientation of S_{Hmax} is subject to an uncertainty of about 20–25°. Formal stress inversions of focal mechanisms (FMF) usually provide a better quality data (Arnold and Townend, 2007; Célérier et al., 2012; Dziewonski and Woodhouse, 1983; Gephart and Forsyth, 1984; Michael, 1987). Seismic data contributes further information about the stress field via the shear wave (SW) splitting method (e.g. Buchbinder, 1985, 1990; Li et al., 1988; Wahlstrom, 1987).

These different methods cover a wide depth range. Geological indicators and overcoring provide near surface information. Borehole breakouts and hydraulic fracturing provide stress indicators from a depth of up to 6 km, and in a few scientific drilling projects to depths in excess of 8 km. Seismic data provide via focal mechanisms and shear wave splitting stress information throughout the brittle crust deeper than 40 km. Borehole breakouts are the major contributor beyond focal mechanisms in the Canadian database (Table 1).

2.2. Stress data compilation

The early plate wide compilations of crustal stress indicators helped researchers to recognize the impact of plate boundary forces on large continental crustal areas, such as the North American Plate (Adams, 1987; Adams and Bell, 1991; Fordjor et al., 1983; Gough et al., 1983; Sbar and Sykes, 1973; Zoback and Zoback, 1980, 1981, 1989, 1991). They came to the conclusion, that the crustal stress field is governed by the same forces driving plate tectonic motion, which are called first order stress sources (Table 2). These are the oceanic ridge push, the slab pull at subduction zones (Forsyth and Uyedaf, 1975; Richardson, 1992; Richardson and Reding, 1991; Zoback, 1992; Zoback and Zoback, 1981; Zoback et al., 1989) in interaction with the mantle driving and resisting forces (e.g. Adams and Bell, 1991; Becker and Faccenna, 2011; Ghosh et al., 2013; Gough, 1984; McGarr, 1982) and resistance along transform faults. Another important source of stress in the lithosphere is the gravitational potential energy (GPE — Ghosh et al., 2009; Humphreys and Coblentz, 2007; Naliboff et al., 2012).

The second and third order stress sources (Heidbach et al., 2007, 2010; Müller et al., 1997; Tingay et al., 2005; Zoback, 1992; Zoback and Mooney, 2003) disturb the observed general stress orientation trend from regional through local to reservoir scale (Table 2). They are in a range of about 100–500 km, for the second and <100 km for the third order stress sources.

2.3. World Stress Map project

A key challenge for regional and global compilation of crustal stress information is the combination of stress indicators that encompass a wide range of methods and sample very different rock volumes

Please cite this article as: Reiter, K., et al., A revised crustal stress orientation database for Canada, Tectonophysics (2014), http://dx.doi.org/10.1016/j.tecto.2014.08.006

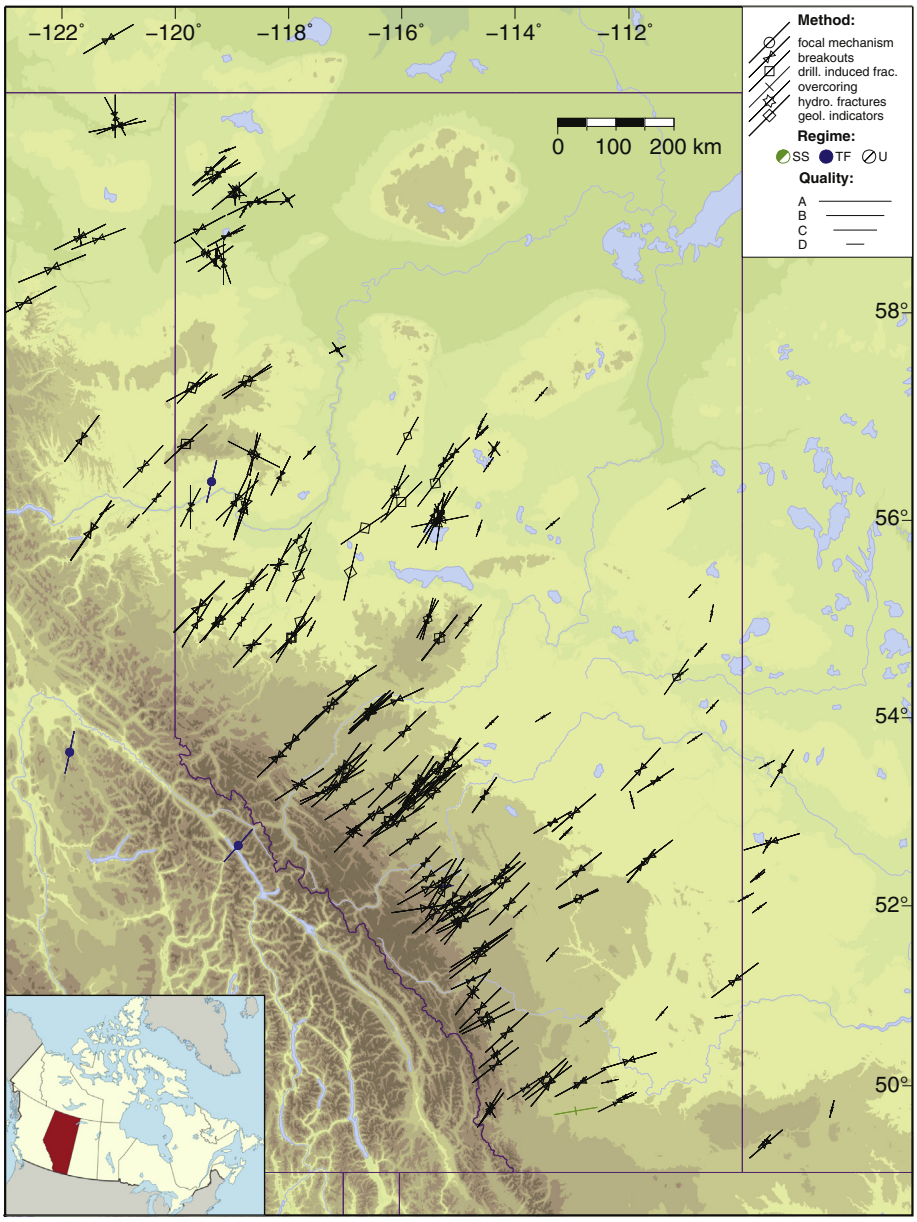

Fig. 3. New stress map of Alberta. Lines represent orientations of maximum horizontal compressional stress (S_{Hmax}), line length is proportional to quality. Colours indicate tectonic stress regimes, with green for strike–slip faulting (SS), blue for thrust faulting (TF), and black for unknown regime (U). The tectonic regime is mostly unknown due to the fact, that only focal mechanisms and overcoring have the potential to derive this information. (For interpretation of the references to colour in this figure legend, the reader is referred to the web version of this article.)

(Ljunggren et al., 2003). In order to make the information comparable, a quality ranking scheme was developed for the World Stress Map project (Zoback, 1992; Zoback and Zoback, 1991; Zoback et al., 1989) and later updated by Sperner et al. (2003) and Heidbach et al. (2009, 2010). The WSM quality ranking scheme is based on the standard deviation on the individual measurements within a given suite. A-quality is the highest and E is the lowest quality. The WSM project website provides a guideline for the data analysis and quality assignment for the WSM database (http://world-stress-map.org).

The first comprehensive global compilation of stress data was initiated by the International Lithosphere Program with the WSM project that published after its first funding phase a database with ~7700 data records (Zoback, 1992). The latest update of the WSM in 2008 has ~21,750 data records (Heidbach et al., 2009, 2010). Nevertheless, data are irregularly distributed across the world with the highest densities coming from sedimentary basins penetrated by many logged boreholes and zones of active seismicity with frequent earthquakes. This unfortunately occurs even in North America, a region with generally many entries, that has large areas with no data due to a lack of oil or gas or mineral exploration or low seismicity. Whatever the application of the data is: analysis of the stress distribution or numerical modelling, the high volume of data in the database reduces uncertainties as well as it allows a better understanding of the local stress field pattern.

2.4. Update of the Canadian Stress map

As crustal stress is not impacted by political boundaries, this update of the Canadian stress map includes data from the northern US and offshore measurements. An artificial boundary is used to compare the amount of existing and updated data records in the database. It is restricted to latitudes ≥41°N as the southern boundary and the longitudes ranging from 142°W to 46°W.

At the beginning of this study, it was first necessary to revise the existing data records according to rigorous application of the latest

Please cite this article as: Reiter, K., et al., A revised crustal stress orientation database for Canada, Tectonophysics (2014), http://dx.doi.org/10.1016/j.tecto.2014.08.006

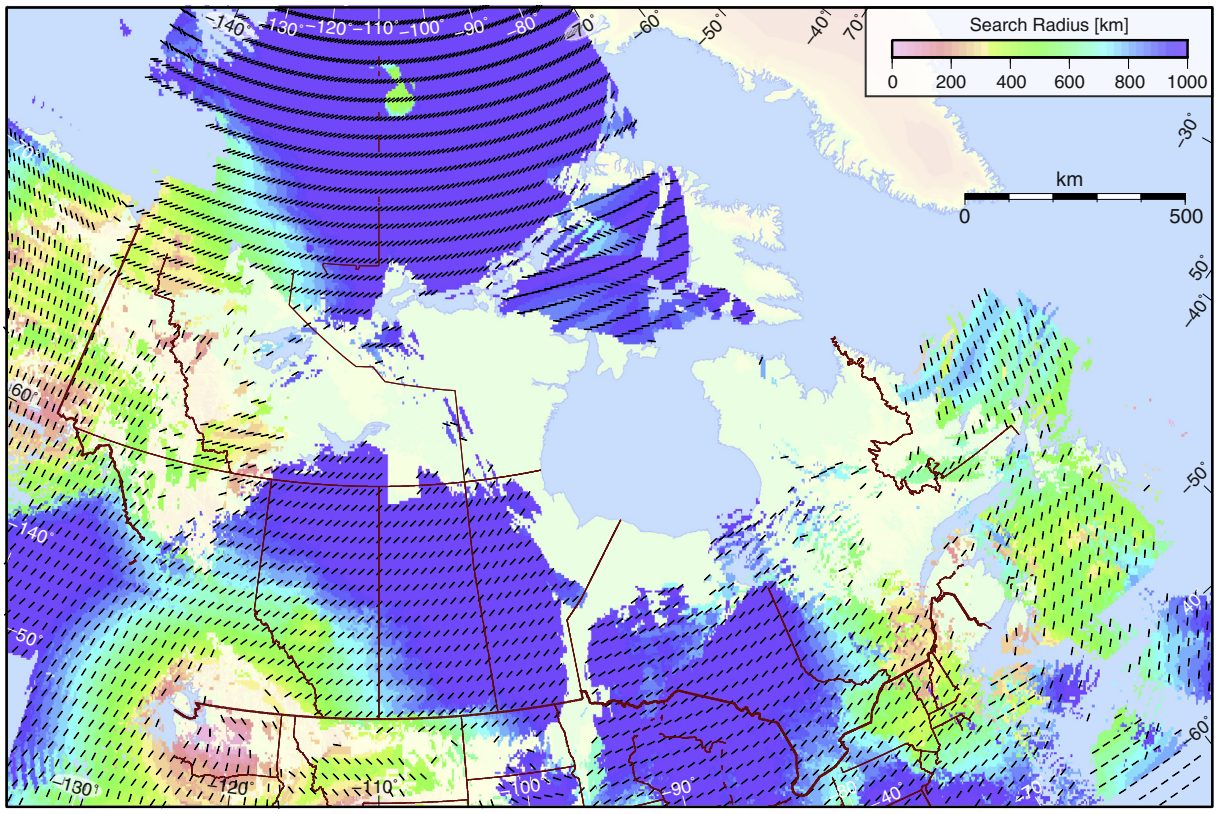

Fig. 4. Wavelength map of Canada and surrounding, results of the statistic stress pattern analysis are displayed. The smoothed S_{Hmax} orientation is visualised by the black strokes, indicating the $\bar{S}_{Hmax}$ azimuths on an 0.75 × 0.75° grid. The largest radii (r_{max}), which fulfil the confidence criteria (QIROC ≤ 20°) and data records n ≥ 5 are colour coded, which is interpreted as the wavelength of the crustal stress pattern. (For interpretation of the references to colour in this figure legend, the reader is referred to the web version of this article.)

revision of the WSM quality ranking (Heidbach et al., 2010), correct of typographical errors, and remove of poor quality data. Data published in the open literature in the 20 years since the first version of the stress map (see below) provided additional information to allow for completion of some of the data records with changes in their quality ranking. In total, 188 data records from the old WSM database were updated.

New data are also added since data published elsewhere and from a previously unavailable dataset that had been maintained by the Alberta Geological Survey (AGS). The published data are compiled from a literature investigation of the following articles by Adams (1987), Balfour et al. (2011), Bell et al. (1994), Bell and Bachu (2003), Buchbinder (1990), Du et al. (2003), Eisbacher and Bielenstein (1971), Hamid (2008), Hurd and Zoback (2012), Konstantinovskaya et al. (2012), Kim (2003), Kim et al. (2006), Ma et al. (2008), Mazzotti and Townend (2010), Michael and Buschkuehle (2008), Ruppert (2008), Steffen et al. (2012), StLouisEQcenter (2010), Yassir and Dusseault (1992), and Zakharova and Goldberg (2014). The update adds up to 514 new records in Canada (Fig. 1) with a grand total of 1667 entries (Fig. 2, Table 1). In Alberta, 78 records were modified and 142 new ones are added to the WSM database; nearly doubling the data set to 297 entries (Fig. 3). This is highly advantageous because it allows for a refinement of the grid and for increased confidence in the application of statistical analysis than before.

3. Statistical analysis of the Canadian stress data

3.1. Mean orientation and wavelength analysis

It is assumed that large intra-plate regions, such as much of Northern America have a uniform S_{Hmax} orientation that is governed by plate boundary- and body forces (Adams, 1987; Adams and Basham, 1989; Adams and Bell, 1991; Fordjor et al., 1983; Gough et al., 1983; Zoback and Zoback, 1980, 1981, 1989, 1991). That said, several intra-plate regions are influenced or disturbed by the second and third order stress sources. As such, it can be difficult to separate the first from the higher order stress.

To better understand such regions, interpolation and smoothing algorithms have been applied in local studies (Bird and Li, 1996; Hansen and Mount, 1990; Heidbach and Ben-Avraham, 2007; Müller et al., 2003; Rebaï et al., 1992). A further motivation of such studies is to fill gaps in the distribution of the data record, which allows estimations of the stress orientation.

The first global statistical stress pattern analysis was carried out by the use of 4527 A–C quality entries from the WSM 1992 database by Coblentz and Richardson (1995). Their statistical test on S_{Hmax} orientations separated the data into 5 × 5° bins. They determined the bins, in which the S_{Hmax} orientation is not randomly distributed, based on a circular confidence level (Mardia, 1972). Depending on different confidence levels, the orientation of the mean S_{Hmax} ($\bar{S}_{Hmax}$) was plotted. Their results suggested a strong correlation between the ridge push and the absolute plate velocity azimuths with the average S_{Hmax} orientation.

A similar analysis is presented by Heidbach et al. (2010) by means of nearly four times the number of data records (16,969 A–C quality data). In contrast to Coblentz and Richardson (1995), they used a reticular node geometry with a spatial resolution of 0.5 × 0.5°, with a variable area around the nodes with radii ranging from 100 to 1000 km. The radius of a given area was successively varied. The $\bar{S}_{Hmax}$ orientation was estimated with a circular standard deviation (SD) (Mardia, 1972) of $\sigma \leq 25°$ thus providing a smoothed global stress map. Their colour coded maps indicate the largest diameter which fulfils the criterion (SD ≤ 25°); these diameters are interpreted as wavelength of a homogeneous stress orientation. Their map confirmed regions with long wavelength pattern (≥1000 km) in North America. The $\bar{S}_{Hmax}$

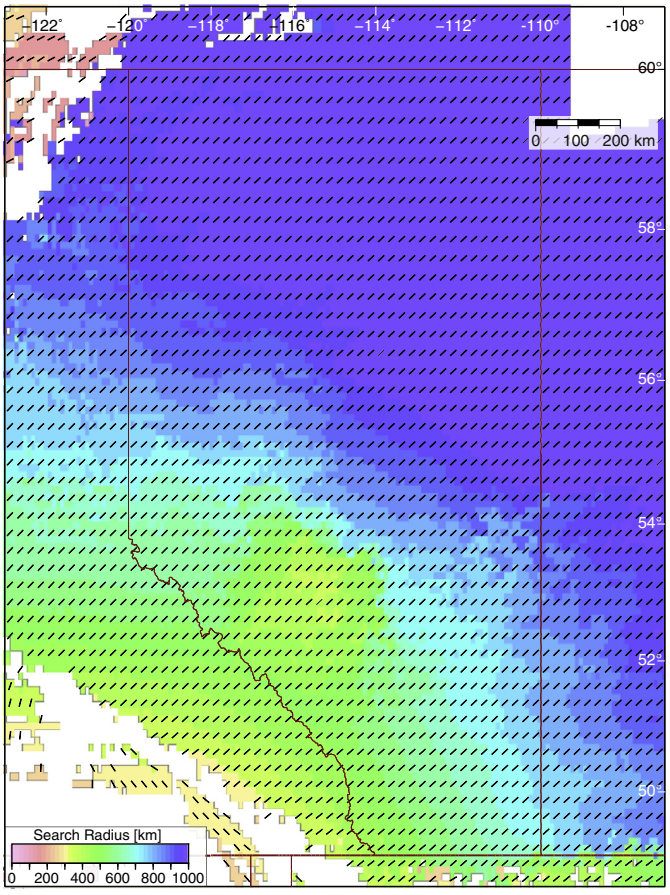

Fig. 5. Wavelength map of Alberta, the average S_{Hmax} orientation is visualised by the black strokes, indicating the $\widetilde{S}_{Hmax}$ azimuths on a 0.25 × 0.25° grid. The largest radii (r_{max}), which fulfil the confidence criteria (QIROC ≤ 20°) and data records n ≥ 5 are colour coded, which is interpreted as the wavelength of the crustal stress pattern. An increasing wavelength, orthogonal to the Rocky Mountains in direction to the Canadian Shield is observed. (For interpretation of the references to colour in this figure legend, the reader is referred to the web version of this article.)

orientations were also compared to the ridge push and absolute plate velocity azimuths.

3.2. Median and quartiles on periodic data

The major problems of circular statistics on stress orientation data are the following: 1. usually there are just a few data records in a certain area, 2. all of these stress indicators have large uncertainties and variation, and 3. the data sets are contaminated with incorrect data (outliers). For example tensile fractures are often misinterpreted as borehole breakouts (e.g. Barton and Moos, 2010; Brudy and Kjørholt, 2001), which results in a 90° rotation in S_{Hmax}. These outliers (3.)) in combination with less data (1.)) could disturb the calculation of the mean drastically.

Therefore, the median is preferred as estimator of the average, because of its robustness in terms of outliers. Based on the Mardia Median (Mardia, 1972) for circular data, and the linear quasi median (Hodges and Lehmann, 1967), Ratanaruamkarn et al. (2009) introduced the quasi median on the circle ($\widetilde{\theta}$):

$$\widetilde{\theta} = \theta_{.50} = \begin{cases} \arctan\left(\dfrac{\sin\theta_{m+1}}{\cos\theta_{m+1}}\right) & \text{if } n = 2m+1 \\ \arctan\left(\dfrac{\sin\theta_m + \sin\theta_{m+1}}{\cos\theta_m + \cos\theta_{m+1}}\right) & \text{if } n = 2m \end{cases} \quad (1)$$

where $\theta_1 < \theta_2 < \cdots < \theta_n$ are the ordered circular data. This circular quasi median is a better estimator of the average than the median, especially when the sample size (n) is small.

To quantify the spread of the data, neither the variance nor standard deviation is a good estimator for possibly contaminated data sets. In such a case the interquartile range (IQR):

$$IQR = Q_{.75} - Q_{.25} \quad (2)$$

is a good estimator of data spreading in the linear case ($Q_{.25}$ = lower quartile and $Q_{.75}$ = upper quartile — Upton and Cook, 1996). Based on the method, to calculate the quasi median on circular data (Ratanaruamkarn et al., 2009), the lower ($\theta_{.25}$) and the upper quartile ($\theta_{.75}$) on circular data are now calculated as follows:

$$\theta_{.25} = \begin{cases} \arctan\left(\dfrac{\sin\theta_{m+1}}{\cos\theta_{m+1}}\right) & \text{if } n = 4m \\ \arctan\left(\dfrac{3\sin\theta_m + \sin\theta_{m+1}}{3\cos\theta_m + \cos\theta_{m+1}}\right) & \text{if } n = 4m+1 \\ \arctan\left(\dfrac{\sin\theta_m + \sin\theta_{m+1}}{\cos\theta_m + \cos\theta_{m+1}}\right) & \text{if } n = 4m+2 \\ \arctan\left(\dfrac{\sin\theta_m + 3\sin\theta_{m+1}}{\cos\theta_m + 3\cos\theta_{m+1}}\right) & \text{if } n = 4m+3 \end{cases} \quad (3)$$

$$\theta_{.75} = \begin{cases} \arctan\left(\dfrac{\sin\theta_{3m+1}}{\cos\theta_{3m+1}}\right) & \text{if } n = 4m \\ \arctan\left(\dfrac{3\sin\theta_{3m} + \sin\theta_{3m+1}}{3\cos\theta_{3m} + \cos\theta_{3m+1}}\right) & \text{if } n = 4m+1 \\ \arctan\left(\dfrac{\sin\theta_{3m} + \sin\theta_{3m+1}}{\cos\theta_{3m} + \cos\theta_{3m+1}}\right) & \text{if } n = 4m+2 \\ \arctan\left(\dfrac{\sin\theta_{3m} + 3\sin\theta_{3m+1}}{\cos\theta_{3m} + 3\cos\theta_{3m+1}}\right) & \text{if } n = 4m+3. \end{cases} \quad (4)$$

The newly introduced quasi interquartile range on the circle (QIROC) is now calculated:

$$QIROC = \theta_{.75} - \theta_{.25}, \quad (5)$$

which is an even better estimator of data spreading for circular data, robust towards outliers, especially for small data sets.

3.3. Applied statistic method

The quasi circular median (Mardia, 1972; Ratanaruamkarn et al., 2009) of S_{Hmax} ($\widetilde{S}_{Hmax}$) and the new quasi interquartile range in the circle (QIROC), which estimates the variability, are calculated, by means of the A–D quality data records in the updated Canadian stress database (Table 1, Fig. 2) on a 0.75, 0.25 and 0.1° square grid of Canada and surrounding. When calculating $\widetilde{S}_{Hmax}$ and the QIROC, the distance and the quality of the measured data were weighted by a quality index according to the scheme of Heidbach et al. (2010). The quality weighting is w_Q = 1/15 for A quality, 1/20 for B quality, 1/25 for C quality, and 1/40 for D quality. Distance (D) weighting w_D = 1/D (D = 25 km when D < 25 km) is applied, where D is the distance from the measured location to the grid point. The largest allowed variability of used data records on a single grid point is limited with a QIROC of ≤20°. The lower limit of data records is n ≥ 5, where n is the number of reliable data records within the search radius.

Beginning with a search radius (r) of 1000 km around each grid point, the radius is reduced stepwise by 100 km down to 200 km, then in 50 km steps down to 50 km and finally 25 km is the smallest search radius. The largest radius, which fulfils all criteria (QIROC ≤ 20°, n ≥ 5) is r_{max}. All data within the largest radii around the grid point are used to calculate $\widetilde{S}_{Hmax}$ orientation. The $\widetilde{S}_{Hmax}$ azimuths are plotted based on the 0.75° grid for Canada (Fig. 4) and with the 0.25° grid for Alberta (Fig. 5).

To visualise the wavelength of homogeneous stress orientations in the maps, r_{max} is plotted colour coded, based on a 0.1 × 0.1° grid for both maps (Figs. 4 and 5). Pink indicates small wavelength <200 km,

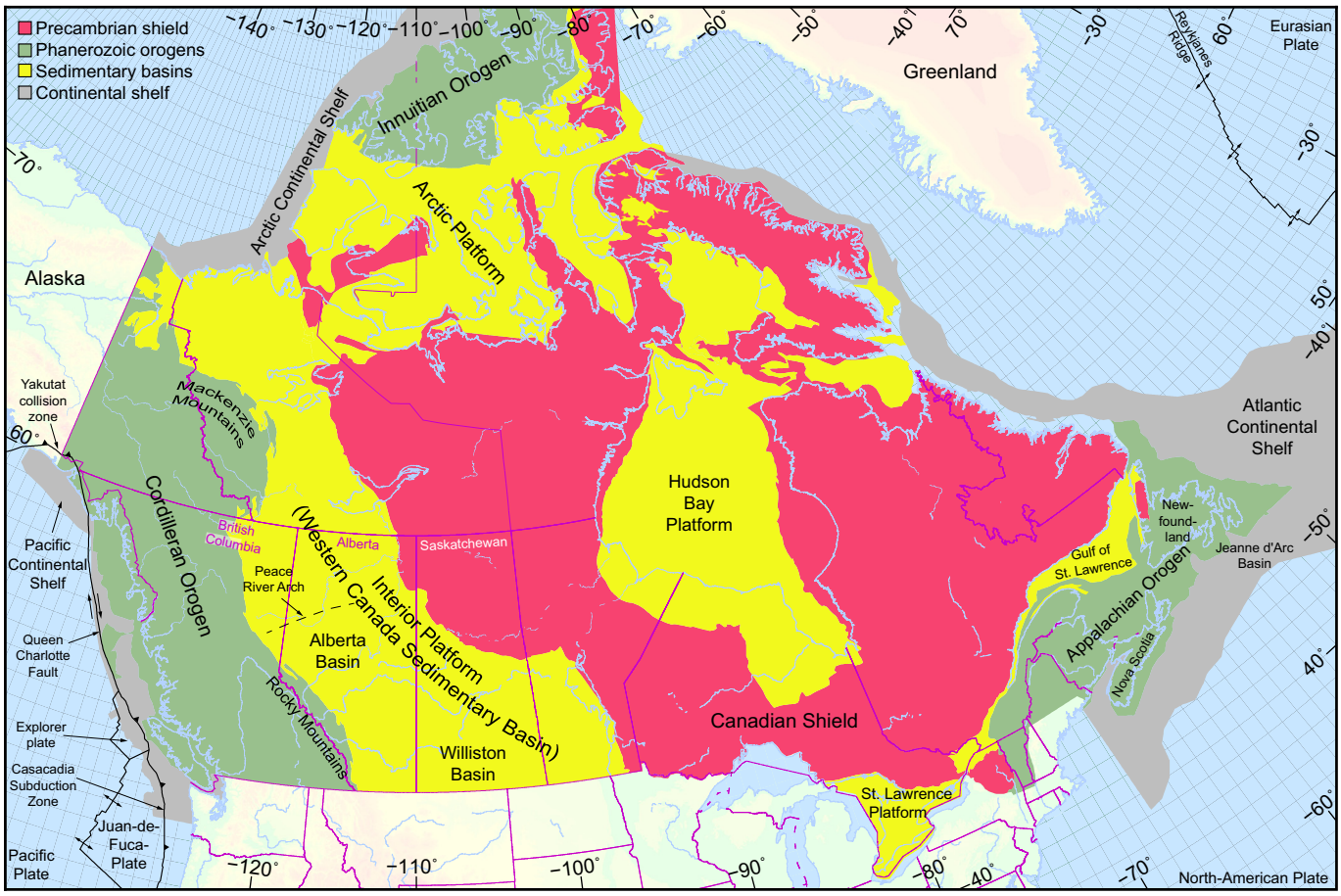

Fig. 6. Map of the Canadian geological provinces, with the main tectonic features. The Canadian Shield (incorporating seven geological provinces) is in red, the platform-sedimentary basins onto the Canadian Shield in yellow, building together the consolidated craton. The Phanerozoic orogens are in green, continental shelf areas in grey. Plate boundaries are taken from the global model PB2002 of Bird (2003), modified and indicated by black, administrative borders by pink lines. The map is redrawn and modified after NRCan (2009). (For interpretation of the references to colour in this figure legend, the reader is referred to the web version of this article.)

green indicates intermediate 400–600 km, and blue indicates long wavelength areas >800 km.

4. Geologic and tectonic setting

For the interpretation of the resulting stress pattern displayed in Figs. 2, 3, 4 and 5, we summarize in the following section the main geological and tectonic setting of Canada and in particular for Alberta.

4.1. Canada

The geological units of Canada (Fig. 6) range from one of the oldest rocks worldwide on the Canadian Archean Shield to young glacial sediments. The main structural unit is the Canadian Shield: a vast composite cratonic region assembled during the late Palaeo-proterozoic (e.g. Hoffman, 1989). It is exposed in the north-central part of North America, mainly to the east and to the west of the Hudson Bay area. The craton is covered by four sedimentary basins. These are the Interior Platform or Western Canadian Sedimentary Basin (WCSB), including the Alberta Basin and the Williston Basin (Porter et al., 1982; Wright et al., 1994), the Arctic Platform to the north and the St. Lawrence Platform to the east. Additionally, the Hudson Bay Platform is located in the centre of the Canadian Shield (e.g. Norris, 1986).

Except the Hudson Bay Platform, each of these platforms is in contact with a Phanerozoic orogenic belt surrounding the Canadian Shield. The oldest is the Palaeozoic Appalachian Orogen on the south-east coast (e.g. Pollock et al., 2012). The Innuitian Orogen (e.g. Oakey and Stephenson, 2008) developed in the north of the Arctic Platform, from Cretaceous to Palaeocene. To the west of the WCSB is a wide Mesozoic to recent mountain chain of the Canadian Cordillera with the front-ranges of the Rocky Mountains riding upwards over the craton (Gabrielse and Yorath, 1989; Monger and Price, 2002; Monger et al., 1972; Price, 1981a, 1986, 1994; Sigloch and Mihalynuk, 2013). Offshore are the Pacific-, the Arctic- and the Atlantic Continental shelves as transition regions to the oceanic crust.

There are two major plate boundaries, which could influence the present stress field in Canada. To the west, the boundary between the North American Plate and the Pacific Plate near the latitude of the Canada–U.S. border is represented by the Cascadian subduction zone. At this contact the Juan-de-Fuca-Plate is subducting eastward under the North American Plate. To the north and nearly parallel to the western shoreline the plate boundary is marked by the south–south-east trending Queen Charlotte transform fault, whereas south of the Cascadian subduction zone, the plate boundary is represented by the San Andreas fault zone. To the East, the Reykjanes Ridge (Mid-Atlantic rift zone) is about 1500 km outboard and sub-parallel to the eastern Canada shoreline.

4.2. Alberta

The Alberta Basin, occupies a portion of the much larger WCSB (Fig. 6) and was formed as a foreland basin during the Middle Jurassic to early Eocene development of Rocky Mountains portion of the Cordilleran foreland fold-and-thrust belt (e.g. Porter et al., 1982; Price, 1981b;

Please cite this article as: Reiter, K., et al., A revised crustal stress orientation database for Canada, Tectonophysics (2014), http://dx.doi.org/10.1016/j.tecto.2014.08.006

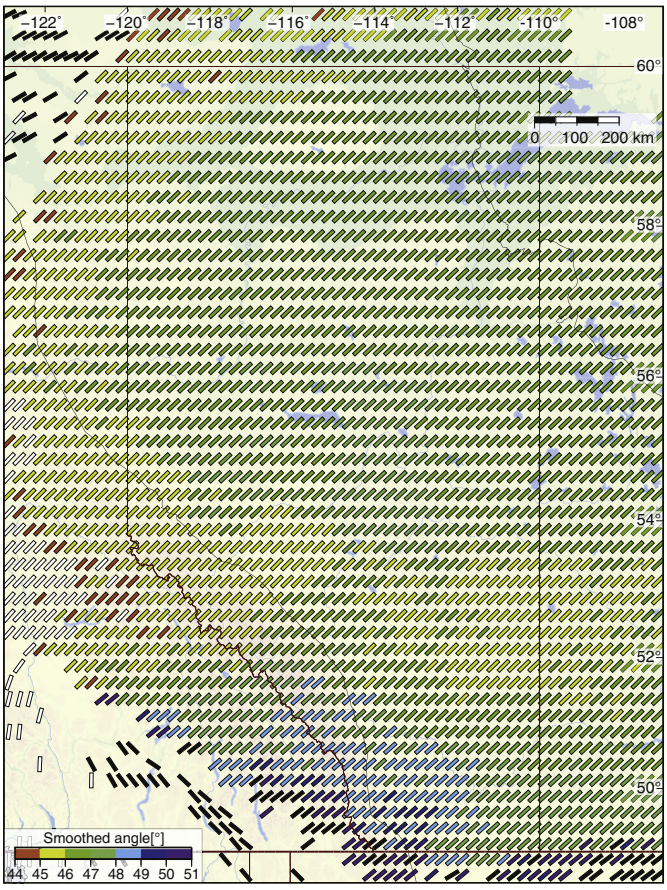

Fig. 7. Map of Alberta, displaying the smoothed S_{Hmax} orientation ($\widetilde{S}_{Hmax}$) grid from Fig. 5 is colour coded depending on the azimuth angle. The border to the Canadian Shield and to the foreland belt is indicated by a black line. The very small change of the orientation in contrast to the change of topography as well the curvature or the front of the Rocky Mountains fold-and-thrust belt in the southern area is obvious. (For interpretation of the references to colour in this figure legend, the reader is referred to the web version of this article.)

Wright et al., 1994). Sediments settled partly discontinuous during the whole Phanerozoic (Mossop and Shetsen, 1994, Chapter 6–26). The crystalline basement of the WCSB, and implicitly that of the superposed Alberta Basin is the North American craton, which is exposed by erosion to the north-east where it is more commonly called the Canadian Shield. Jurassic to Palaeocene strata deposited in the western part of the Alberta Basin have been incorporated in the Rocky Mountains fold-and-thrust belt, which is bound farther west in British Columbia by the Rocky Mountain Trench. The Alberta Basin consists of an undeformed sedimentary wedge that increases in thickness from zero at the Canadian Shield to approximately 5500 m near the fold-and-thrust belt.

The final shape of the Alberta Basin developed by downward flexing of the Canadian Shield due to lithospheric loading and isostatic flexure in a retro-arc setting (English and Johnston, 2004), together with the sediment derived from the developing Canadian Cordillera. The fold-and-thrust belt documents the deformation history and is curved convexly towards the foreland sedimentary basin. The axis of the fold-and-thrust belt changes orientation from southerly in the northern segment between 60° and 55°N, to south-easterly between 55° and 49°N, and again to southerly close to the U.S. border. These orientation changes of about 30°, includes the peculiar convex curvature of the fold-and-thrust belt in southern Canada was variously assigned to either changing stresses at the plate boundary, or a re-entrant in the ancestral margin of north America (north of the Montania promontory, see McMechan and Price, 1982).

5. Results and discussion

5.1. $\widetilde{S}_{Hmax}$ orientation and QIROC as new statistical methods

Statistical methods, to determine a grid with average S_{Hmax} orientations are further developed in this paper, based on Coblentz and Richardson (1995) and Heidbach et al. (2010). A circular median S_{Hmax} ($\widetilde{S}_{Hmax}$) is a better estimator of the S_{Hmax} orientation than the circular mean S_{Hmax} ($\overline{S}_{Hmax}$), because $\widetilde{S}_{Hmax}$ is more robust to outliers. The allowed deviation criteria, a standard deviation of $\leq 25°$, used from Heidbach et al. (2010) is replaced by the quasi interquartile range on the circle (QIROC $\leq 20°$), which is more strict. This may exclude some data records, but in general it gives a more precise and robust estimator, which is justified by the increasing amount of available data. However, despite the fact, that orientation data are weighted according the quality ranking scheme, uncertainties are not eliminated. Especially systematic errors are reproduced by the method, whereas random errors are balanced.

The resolution of the used rectangular grid (0.75°) of smoothed S_{Hmax} orientation in Canada (Fig. 4) is slightly coarser then the grid used by Heidbach et al. (2010) and seven times finer than the grid used by Coblentz and Richardson (1995). For the Alberta map (Fig. 5), the grid resolution (0.25°) is two times and 20 times finer, respectively. The colour coded grid of the wavelength (0.1°) has a five times higher resolution than that one used by Heidbach et al. (2010). The general $\widetilde{S}_{Hmax}$ orientation is similar to the previously found $\overline{S}_{Hmax}$ orientation (Coblentz and Richardson, 1995; Heidbach et al., 2010), but with a higher resolution, a better coverage and smaller confidence level.

5.2. Stress pattern in Canada

It is assumed that first order stress sources like ridge push, slab pull, mantle tractions and gravitational potential energy (GPE) are the main drivers of the stress field in the North American crust (Adams, 1987; Adams and Basham, 1989; Adams and Bell, 1991; Flesch et al., 2007; Fordjor et al., 1983; Ghosh et al., 2013; Gough, 1984; Gough et al., 1983; Humphreys and Coblentz, 2007; McGarr, 1982; Richardson and Reding, 1991; Sbar and Sykes, 1973; Zoback, 1992; Zoback and Zoback, 1980, 1981, 1989). The overall observed S_{Hmax} orientation is about north-east. According to the assumed second order stress sources (Adams and Basham, 1989; Adams and Bell, 1991; Zoback, 1992), the following influences are suggested to act in Canada: isostatic rebound as reaction to the load of thick ice sheets during ice age, margin-normal extensional stresses on the continental shelf and margin-normal compressional stresses in the adjacent oceanic part. The latter two influences could be the case for the Atlantic margin. Proterozoic or Palaeozoic suture zones as well other structures should not or only slightly disturb the recent plate driven stress field (Zoback, 1992). According to Camelbeeck et al. (2013), the orientation of the stress field could be estimated as perpendicular to the slope of the geoid high. Comparison of the geoid heights (Huang and Véronneau, 2005) with the stresses fit for the Rocky Mountains in Alberta. But for whole Canada (Véronneau, 1997), the correlation of the observed stress pattern vs. geoid high is not convincing. But the stress pattern is consistent with estimations of crustal stress by GPE models (Flesch et al., 2007) in western Canada.

The Stress Map of Canada (Fig. 2) displays several regions with a very dense net of in-situ stress data but still has wide regions with no or just a few observations. The majority of the data records are focal mechanisms (46%, n = 767) and from borehole breakouts (39%, n = 657), see Table 1. Focal mechanisms are concentrated on the east coast at the St. Lawrence Platform and along the Appalachian Orogen as well as offshore of the west coast, along the Cascadian subduction zone and the Queen Charlotte fault (Fig. 2). Borehole breakouts in contrast are mainly eastward of the Canadian Cordillera and in the Atlantic continental shelf

Please cite this article as: Reiter, K., et al., A revised crustal stress orientation database for Canada, Tectonophysics (2014), http://dx.doi.org/10.1016/j.tecto.2014.08.006

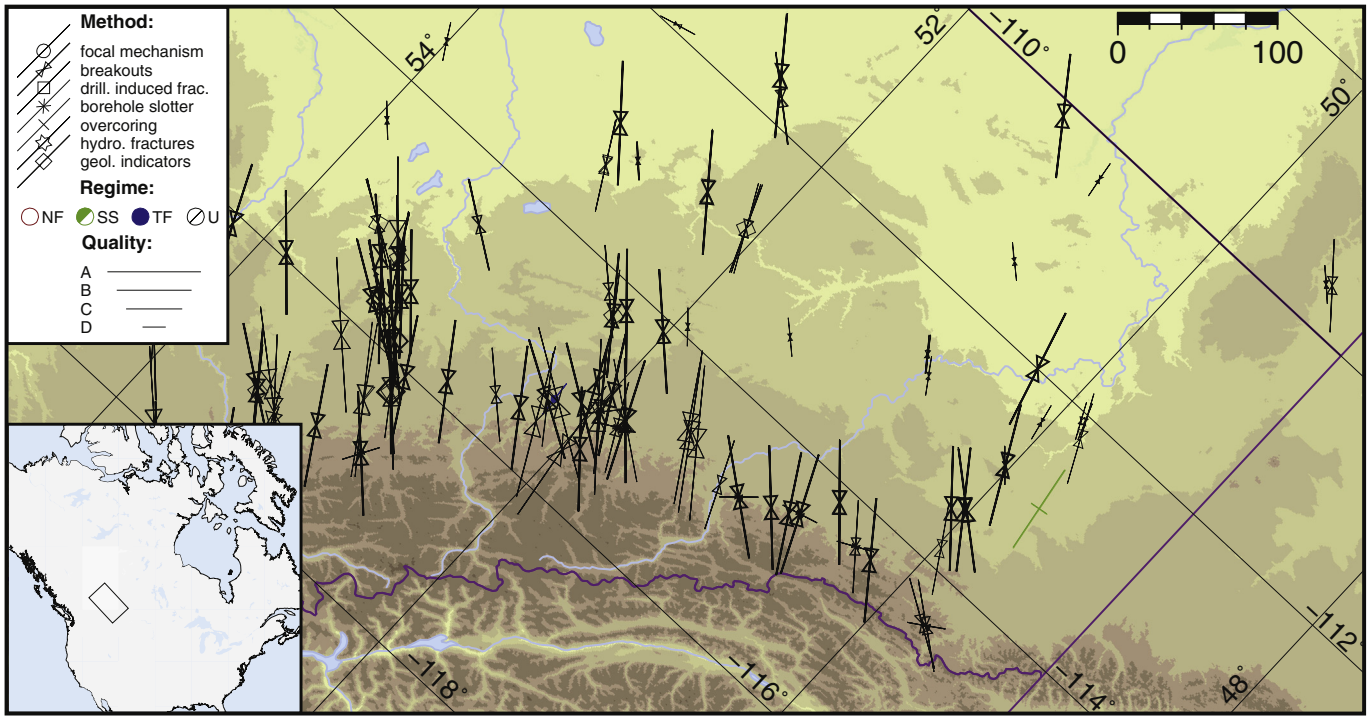

Fig. 8. Part of the Alberta Stress Map, rotated about 47° counter-clockwise. The map displays, that S_{Hmax} orientation does not always follow perpendicular the topographic trend, which is in contrast to the S_{Hmax} orientation, which is to observe in the Alpine Molasse basin (Fig. 9).

area along the east coast. Substantial portions of the data are from the Alberta Basin to the east of the Rocky Mountain trench.

There is a general trend of the S_{Hmax} orientation east of the Cordillera towards northeast–southwest, visible in Fig. 2. A similar pattern is visible for $\tilde{S}_{Hmax}$ (Fig. 4); the smoothed S_{Hmax} is also preferentially oriented northeast–southwest in most regions. The strong correlation of S_{Hmax} orientation in the mid-plate crust of North America with plate motion (Henton et al., 2006) has been interpreted to be due to resistive drag at the base of the plate (Adams and Basham, 1989; Adams and Bell, 1991; Gough, 1984; Gough et al., 1983; Zoback et al., 1989). This orientation is also in the expected orientation based on Mid-Atlantic push (Zoback et al., 1989, and references therein).

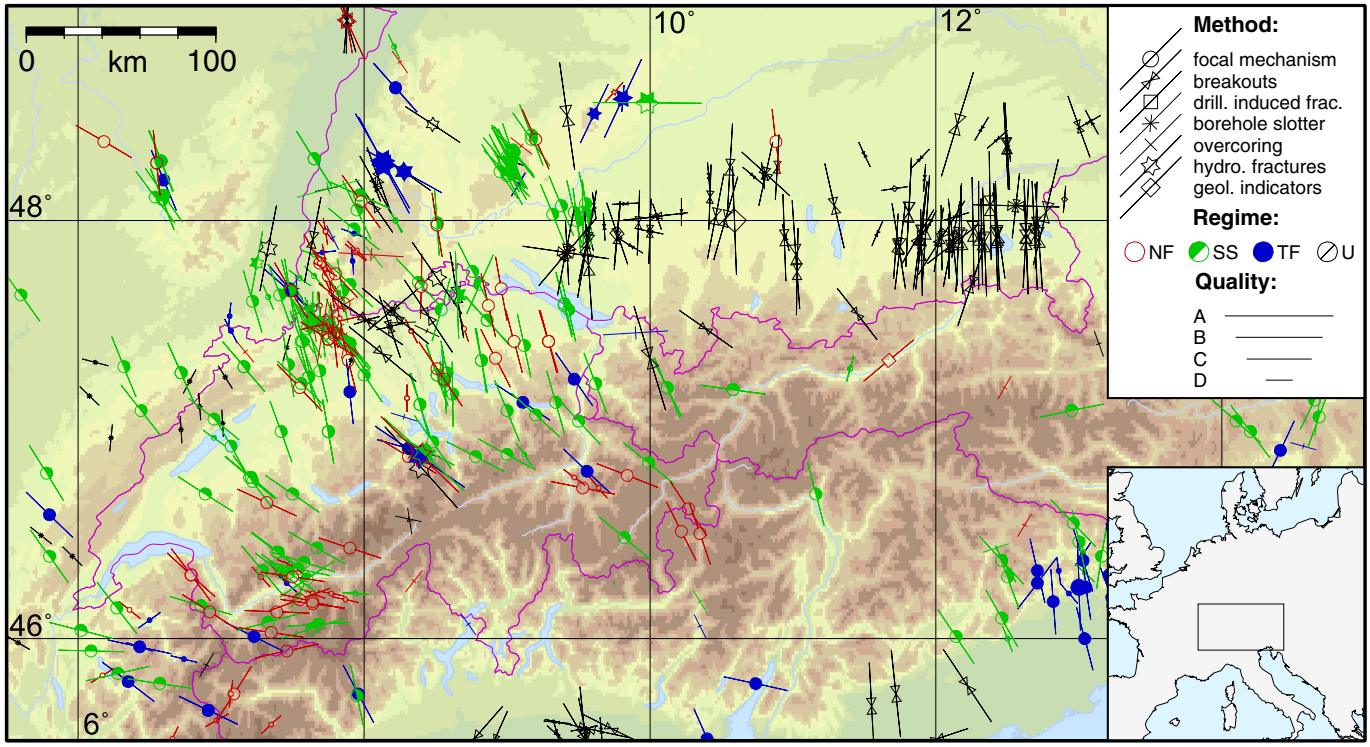

Fig. 9. Stress map of the Alpine Molasse basin. S_{Hmax} orientation follows perpendicular the topographic trend of the Alpine Mountain chain.

Please cite this article as: Reiter, K., et al., A revised crustal stress orientation database for Canada, Tectonophysics (2014), http://dx.doi.org/10.1016/j.tecto.2014.08.006

The wavelength map of Canada (Fig. 4) displays long wavelengths in the area of the Canadian Shield (Fig. 6) and a transition to intermediate wavelengths in the areas of the sedimentary basins onto the Canadian Shield. On the east coast, the foothills of the Appalachian Mountains as well as the continental shelf areas are characterized by intermediate to small wavelengths. In the most parts of the Canadian Cordillera, short wavelengths are observed. There are some regions where the wavelength map displays long wavelengths, for example in Saskatchewan, where only a few stress orientation indicators are measured. This is due to the homogeneous stress data, when large search radii fulfil the pass criteria. On the other hand some regions with a few measurements display no wavelength, as the pass criteria is not fulfilled. The data points from the Hudson Bay for example illustrates this perfectly: there are five data points (Fig. 2), but one of them have clearly a larger deviation than the defined QIROC of ≤20° for at least necessarily data points ($n \geq 5$), to fulfil the criteria.

The stress orientation is different in the north-western Canadian Cordilleras, where $\widetilde{S}_{Hmax}$ points to the north. This is associated to the transform plate boundary between the North American Plate and the Pacific Plate. This trend continues but rotates to a south-east orientation of S_{Hmax} in northern Alaska, as discussed in Adams and Basham (1989), Adams and Bell (1991).

Only in the Mackenzie Mountains, north of the Rocky Mountains, the $\widetilde{S}_{Hmax}$ orientation changes from north-east to north, this rotation has also been observed by Ristau et al. (2007). The majority of the S_{Hmax} azimuth data are oriented perpendicular to the topography of the Mackenzie Mountains and follow nicely the curved shape of those mountains with a rotation of nearly 90°. Besides the topographic effect, this also may be caused by a north to south oriented strike slip zone and a proposed strain transfer from the Yakutat collision zone by a lower crustal detachment (Mazzotti and Hyndman, 2002).

Within the Hudson Bay, Bell and Wu (1997) observed S_{Hmax} orientation to the north-east, according the overall trend, which is observed in both sub-salinary and supra-salinary sediments. North of the Hudson Bay area S_{Hmax} orientations are towards south-east. These orientations are derived from only a few focal mechanisms. These deviations from the overall stress pattern can be possibly explained by post-glacial isostatic rebound (Adams and Basham, 1989; Adams and Bell, 1991). However, elastic thickness in the centre of the Canadian Shield is 80 km (Kirby and Swain, 2014), but the inner part of the Canadian Shield has V_S velocities constantly lower than in the outer rim (Kao et al., 2013). Perhaps these structures explain even better that several of the S_{Hmax} data are oriented towards the centre of the Canadian Shield, even for northward oriented data in the south of the Hudson Bay.

Along the St. Lawrence Platform up to the Gulf of St. Lawrence and in the northern part of the Appalachian Mountains, the S_{Hmax} orientations are inhomogeneous and the wavelengths are short, partly <50 km. A possible reason for this may be that the earthquakes, from which the S_{Hmax} orientations are derived, occurred on a fault system that is not optimally oriented in the contemporary stress field. Following Heidbach et al. (2010), FMS data always have the potential to inherit larger uncertainties on the derived S_{Hmax} orientation than indicated by the C-quality assigned by default (Célérier et al., 2012). Another explanation is a low velocity anomaly, observed in shallow depth (<20 km) (Kao et al., 2013). However, stress orientations in this region are most probably perturbed by the second or third order stress sources such as low friction faults and less from isostatic rebound (Mazzotti and Townend, 2010).

The orientation of S_{Hmax} along the south-eastern coast is sub-parallel to the shore line, which indicates that neither sedimentary load on the shelf nor buoyancy contrast on the continental slope disturbs the overall stress pattern. Some irregularities are observed south-east of Nova Scotia. In this region a ductile salt layer and an over-pressured zone are accused to affect the general stress pattern (Yassir and Bell, 1994). Bell (1996) interprets the irregular stress pattern in the Jeanne d'Arc Basin offshore Newfoundland by the same overprint mechanism.

The stress pattern in the shelf area to the north of the Gulf of St. Lawrence is more irregular. S_{Hmax} orientations in the region between Alaska and Greenland are north–northeast oriented, which neither fits to the overall stress pattern (north-east) nor to the orientation of the continental slope, which is also north-east. Zoback et al. (1989) and Zoback (1992) suggest, that some regions seems to be partly superimposed by local stress perturbation due to the sedimentary load, loading flexure or other sediment related effects along the continental shelf.

5.3. Stress pattern in the Alberta Basin

The stress field over much of Alberta has been studied for more than 30 years (e.g. Fordjor et al., 1983; Gough et al., 1983; Bell et al., 1994) with stress orientations obtained from nearly all of Alberta except for the north-east (Fig. 3). There are some zones of clustered data that come from areas where appropriate borehole log data was available. Visual inspection of the map indicates a rather homogeneous pattern of north-east directed stress orientations that are approximately perpendicular to the Rocky Mountain orogenic belt. A slight change of the orientation may follow the large scale curvature of the Rocky Mountain range in southern Alberta and is in agreement to the previous studies (e.g. Bell et al., 1994; Fordjor et al., 1983; Gough et al., 1983). The stress orientations in the Alberta Basin are consistent within single stratigraphic units (Bell and Bachu, 2003) and down across several stratigraphic levels to the Precambrian basement (Bell, 1996; Bell and Grasby, 2012; Fordjor et al., 1983). This average stress orientation (north-east) is concurrent to the observed overall pattern in Canada.

The median S_{Hmax} ($\widetilde{S}_{Hmax}$) orientation (Fig. 5) in Alberta is very uniform and on casual inspection appears constant everywhere. To highlight more subtle variations of the $\widetilde{S}_{Hmax}$ azimuth in Alberta the angle of the $\widetilde{S}_{Hmax}$ orientations is colour coded in Fig. 7. These orientations range from only 45–47° over most of Alberta, and deviate from this trend only in the south-west where the angle rotates to 51°. Therefore the $\widetilde{S}_{Hmax}$ orientation varies only a few degrees.

Fig. 8 displays the S_{Hmax} orientation in the southern Alberta Basin. In the very south at 50°N of the Rocky Mountains it is convexly curved, but the stress orientation in the foothills and the Alberta Basin do not follow this trend, This is in contrast to the assumption from Bell and Gough (1979) and to comparable tectonic settings like the Molasse Basin of Germany, immediately north of the European Alps (Fig. 9). In the curved Molasse foreland basin, the S_{Hmax} orientations are consistently perpendicular to the topography (Reinecker et al., 2010). The S_{Hmax} orientation there follows nicely the basin geometry and the crustal thickness. The cause could be the different age of the foreland basin's development. The younger Molasse basin developed in the Cenozoic whereas the Alberta Basin is a result of Mesozoic deformation. An end-member in such a train of thought is the Palaeozoic Appalachian Mountains (Fig. 2), where S_{Hmax} neither shows any context to past orogenic shortening nor to recent topography.

In southern Alberta, the influence of the topography and the curved fold-and-thrust belt are limited on the stress orientations. This suggests that deeper effects such as the influence of basal tractions from density driven mantle convection (e.g. Becker and Faccenna, 2011) or the influence of lithospheric thickness and density variations may predominate (e.g. Camelbeeck et al., 2013; Flesch et al., 2007; Naliboff et al., 2012). Recent modelling of upper crustal stress orientation and magnitude in the Alberta Basin demonstrates less influence of Mohorovičić depth-variation below the Rocky Mountains (Reiter and Heidbach, 2014).

In contrast to the Canadian map, the colour coded wave-length map of Alberta (Fig. 5) displays no gaps. It changes from intermediate wavelengths (~400 km) in the Rocky Mountains region (with only three focal mechanisms) and ingresses perpendicular to Rocky Mountains up to large wavelengths (>1000 km) in the area of the Canadian Shield, but also in the northern part of the Alberta Basin. Small wavelengths in the Rocky Mountains are caused by the variable orientation of focal

Please cite this article as: Reiter, K., et al., A revised crustal stress orientation database for Canada, Tectonophysics (2014), http://dx.doi.org/10.1016/j.tecto.2014.08.006

mechanisms in Washington State in the US due to the subduction of the Juan-de-Fuca-Plate below the North America Plate.

There are just a few orientation data, differing from the main trend like those close to the Peace River Arch, (about 56°N in Fig. 3), where a counter-clockwise rotation of about 20° is observed. The Peace River Arch has an elevated Precambrian basement (Bell and Grasby, 2012; Halchuk and Mereu, 1990), which could be interpreted as a buried contractional duplex. The other explanations for the locally perturbed stress field in the Peace River region are mafic sills, which intruded in the upper crust (Eaton et al., 1999) and/or lateral heterogeneities (transfer zone or local rheological properties), according to Bell and McCallum (1990). Dusseault and Yassir (1994) modelled successfully the stress perturbation in the Peace River Arch with an anisotropic softer inclusion.

The variation of S_{Hmax} azimuths in Alberta (e.g. Bell and Babcock, 1986; Bell et al., 1994) or the last WSM update by Heidbach et al. (2010), when comparing visually with this update (Fig. 3), seems to be decreasing. This is confirmed by a change of the circular (non-rated) standard deviation (Mardia, 1972) from 9.2°, for the old Alberta WSM dataset to a standard deviation of 8.7° for the new complete Alberta dataset. This shows that an increasing amount of available data records and the stringent application of common quality criteria reduce uncertainties, at least for Alberta.

6. Conclusion

The maximum horizontal crustal stress (S_{Hmax}) is oriented southwest to north-east over wide areas in Northern America. However, there was no systematic revision or extension on the Canadian stress database for about two decades (Adams and Bell, 1991; Bell et al., 1994); the data records in the WSM 2008 release (Heidbach et al., 2010) included 1153 S_{Hmax} orientation data. The WSM database for Canada has now been completely revised and 514 new data records were added, with a special emphasis on Alberta. The data are from intra-plate regions as well as from plate boundaries and sedimentary basins. The new Canadian stress database with now 1667 data records is more reliable since all data records are cross checked with common modern WSM quality criteria. The largest accession occurred in Alberta and in the south-eastern region (St. Lawrence Platform and Appalachian Orogen). Furthermore, the high data density allows a robust assessment and interpretation of the S_{Hmax} orientation. This is important for the data application for statistic smoothing algorithms or for the validation of geomechanical models.

The Alberta region displays a uniform S_{Hmax} orientation (~47°N) with a clear increase of wavelength in the same orientation, towards the Canadian Shield. In contrast, the region of the Gulf of St. Lawrence Platform and Appalachian Orogen have short to very short wavelengths.

The quasi median on the circle ($\widetilde{S}_{Hmax}$) from (Ratanaruamkarn et al., 2009) that we use to estimate the average S_{Hmax} orientation and the newly introduced equation, to calculate the quasi interquartile range on the circle (QIROC), which estimates the variance of the data, is more robust to outliers within small datasets of periodic data than previously applied techniques. The general smoothed S_{Hmax} orientation is similar to the previously found orientation by Coblentz and Richardson (1995), Heidbach et al. (2010), but with a higher resolution, a better coverage and larger confidence level.

Acknowledgement

This study was conducted under the Helmholtz-Alberta-Initiative (HAI), the first author is grateful for the financial support (SO-061). We also want to thank the Alberta Geological Survey (AGS), which provided the S_{Hmax} data set and allowed us to publish these data in the World Stress Map. Finally we thank two anonymous reviewers, who improved the paper's quality. Maps were generated by means of GMT software (Wessel et al., 2013).

Appendix A. Supplementary data

Supplementary data to this article can be found online at http://dx.doi.org/10.1016/j.tecto.2014.08.006.

References

Aadnøy, B.S., Bell, J.S., 1998. Classification of drilling-induced fractures and their relationship to in-situ stress directions. Log Anal. 39 (December), 27–42.
Adams, J.J., 1987. Canadian crustal stress data: a compilation to 1987. Technical ReportGeological Survey of Canada.
Adams, J.J., Basham, P., 1989. The seismicity and seismotectonics of Canada east of the Cordillera. Geosci. Can. 16 (1), 3–16.
Adams, J.J., Bell, J.S., 1991. Crustal stresses in Canada. In: Slemmons, D.B., Engdahl, E.R. (Eds.), Neotectonics of North America, Decade of North American Neotectonics of North America. Geological Society of America, pp. 367–386.
Amadei, B., Stephansson, O., 1997. Rock Stress and Its Measurement. Chapman & Hall, London.
Angelier, J., 1979. Determination of the mean principal directions of stresses for a given fault population. Tectonophysics 56 (3–4), T17–T26.
Angelier, J., 1984. Tectonic analysis of fault slip data sets. J. Geophys. Res. 89 (B7), 5835–5848.
Arnold, R., Townend, J., 2007. A Bayesian approach to estimating tectonic stress from seismological data. Geophys. J. Int. 170 (3), 1336–1356.
Babcock, E.A., 1978. Measurement of subsurface fractures from dipmeter logs. AAPG Bull. 62 (7), 1111–1126.
Bachu, S., Haug, K., Michael, K., 2008. Stress regime at acid-gas injection operations in western Canada. Energy Resources Conservation Board, ERCB/AGS Special Report 094,pp. 1–49.
Balfour, N.J., Cassidy, J.F., Dosso, S.E., Mazzotti, S., 2011. Mapping crustal stress and strain in southwest British Columbia. J. Geophys. Res. 116 (B3), B03314.
Barton, C.A., Moos, D., 2010. Geomechanical wellbore imaging: key to managing the asset life cycle. Technical ReportGeoMechanics International.
Becker, T.W., Faccenna, C., 2011. Mantle conveyor beneath the Tethyan collisional belt. Earth Planet. Sci. Lett. 310 (3–4), 453–461.
Bell, J.S., 1996. In situ stresses in sedimentary rocks (part 2): applications of stress measurements. Geosci. Can. 23 (3), 135–153.
Bell, J.S., Babcock, E.A., 1986. The stress regime of the Western Canadian Basin and implications for hydrocarbon production. Bull. Can. Petrol. Geol. 34 (3), 364–378.
Bell, J.S., Bachu, S., 2003. In situ stress magnitude and orientation estimates for Cretaceous coal-bearing strata beneath the plains area of central and southern Alberta. Bull. Can. Petrol. Geol. 51 (1), 1–28.
Bell, J.S., Bachu, S., 2004. In-situ stress magnitudes in the Alberta basin-regional coverage for petroleum engineers. Proceedings of Canadian International Petroleum Conference. Society of Petroleum Engineers, Calgary, pp. 1–12.
Bell, J.S., Gough, D.I., 1979. Northeast–southwest compressive stress in Alberta evidence from oil wells. Earth Planet. Sci. Lett. 45 (2), 475–482.
Bell, J.S., Grasby, S.E., 2012. The stress regime of the Western Canadian Sedimentary Basin. Geofluids 12 (2), 150–165.
Bell, J.S., McCallum, R., 1990. In situ stress in the Peace River Arch area, Western Canada. Bull. Can. Petrol. Geol. 38 (1), 270–281.
Bell, J.S., Wu, P., 1997. High horizontal stresses in Hudson Bay, Canada. Can. J. Earth Sci. 34 (7), 949–957.
Bell, J.S., Price, R.A., McLellan, P.J., 1994. In-situ stress in the Western Canada Sedimentary Basin. In: Mossop, G.D., Shetsen, I. (Eds.), Geological Atlas of the Western Canada Sedimentary Basin. Canadian Society of Petroleum Geologists and the Alberta Research Council, pp. 439–446 (chapter 29).
Bird, P., 2003. An updated digital model of plate boundaries. Geochem. Geophys. Geosyst. 4 (3), 1027.
Bird, P., Li, Y., 1996. Interpolation of principal stress directions by nonparametric statistics: global maps with confidence limits. J. Geophys. Res. 101 (B3), 5435–5443.
Brudy, M., Kjørholt, H., 2001. Stress orientation on the Norwegian continental shelf derived from borehole failures observed in high-resolution borehole imaging logs. Tectonophysics 337 (1–2), 65–84.
Buchbinder, G.G.R., 1985. Shear-wave splitting and anisotropy in the Charlevoix Seismic Zone, Quebec. Geophys. Res. Lett. 12 (7), 425–428.
Buchbinder, G.G.R., 1990. Shear wave splitting and anisotropy from the aftershocks of the Nahanni, Northwest Territories, Earthquakes. J. Geophys. Res. 95 (B4), 4777–4785.
Camelbeeck, T., de Viron, O., Van Camp, M., Kusters, D., 2013. Local stress sources in Western Europe lithosphere from geoid anomalies. Lithosphere 5 (3), 235–246.
Célérier, B., Etchecopar, A., Bergerat, F., Vergely, P., Arthaud, F., Laurent, P., 2012. Inferring stress from faulting: from early concepts to inverse methods. Tectonophysics 581, 206–219.
Coblentz, D.D., Richardson, R.M., 1995. Statistical trends in the intraplate stress field. J. Geophys. Res. 100 (B10), 20245–20255.
Cox, J., 1972. The high-resolution dipmeter reveals dip-related borehole and formation characteristics. J. Can. Pet. Technol. 11 (1), 46–57.
Du, W.-x., Kim, W.-Y., Sykes, L.R., 2003. Earthquake source parameters and state of stress for the northeastern United States and southeastern Canada from analysis of regional seismograms. Bull. Seismol. Soc. Am. 93 (4), 1633–1648.
Dusseault, M.B., Yassir, N.A., 1994. Effects of rock anisotropy and heterogeneity on stress distributions at selected sites in North America. Eng. Geol. 37 (3–4), 181–197.
Dziewonski, A.M., Woodhouse, J.H., 1983. An experiment in systematic study of global seismicity: centroid-moment tensor solutions for 201 moderate and large earthquakes of 1981. J. Geophys. Res. 88 (B4), 3247–3271.

Please cite this article as: Reiter, K., et al., A revised crustal stress orientation database for Canada, Tectonophysics (2014), http://dx.doi.org/10.1016/j.tecto.2014.08.006

Eaton, D.W., Ross, G.M., Hope, J., 1999. The rise and fall of a cratonic arch: a regional seismic perspective on the Peace River Arch, Alberta. Bull. Can. Petrol. Geol. 47 (4), 346–361.

Eisbacher, G.H., Bielenstein, H.U., 1971. Elastic strain recovery in Proterozoic rocks near Elliot Lake, Ontario. J. Geophys. Res. 76 (8), 2012–2021.

Ekstrom, M., Dahan, C., Chen, M., Lloyd, P., Rossi, D., 1987. Formation imaging with microelectrical scanning arrays. Log Anal. 28 (3), 13.

English, J.M., Johnston, S.T., 2004. The Laramide orogeny: what were the driving forces? Int. Geol. Rev. 46 (9), 833–838.

Flesch, L.M., Holt, W.E., Haines, A.J., Wen, L., Shen-Tu, B., 2007. The dynamics of western North America: stress magnitudes and the relative role of gravitational potential energy, plate interaction at the boundary and basal tractions. Geophys. J. Int. 169 (3), 866–896.

Fordjor, C.K., Bell, J.S., Gough, D.I., 1983. Breakouts in Alberta and stress in the North American plate. Can. J. Earth Sci. 20 (9), 1445–1455.

Forsyth, D.W., Uyedaf, S., 1975. On the relative importance of the driving forces of plate motion. Geophys. J. Int. 43 (1), 163–200.

Gabrielse, H., Yorath, C., 1989. The Cordilleran orogen in Canada. Geosci. Can. 16 (2), 67–83.

Gephart, J.W., Forsyth, D.W., 1984. An improved method for determining the regional stress tensor using earthquake focal mechanism data: application to the San Fernando Earthquake Sequence. J. Geophys. Res. 89 (B11), 9305.

Ghosh, A., Holt, W.E., Flesch, L.M., 2009. Contribution of gravitational potential energy differences to the global stress field. Geophys. J. Int. 179 (2), 787–812.

Ghosh, A., Holt, W.E., Wen, L., 2013. Predicting the lithospheric stress field and plate motions by joint modeling of lithosphere and mantle dynamics. J. Geophys. Res. Solid Earth 118 (1), 346–368.

Gough, D.I., 1984. Mantle upflow under North America and plate dynamics. Nature 311 (5985), 428–433.

Gough, D.I., Fordjor, C.K., Bell, J.S., 1983. A stress province boundary and tractions on the North American plate. Nature 305 (5935), 619–621.

Haimson, B.C., Fairhurst, C., 1969. In-situ stress determination at great depth by means of hydraulic fracturing. The 11th U.S. Symposium on Rock Mechanics (USRMS), 16–19 June, Berkeley, California. American Rock Mechanics Association, pp. 559–584.

Haimson, B.C., Song, I., 1993. Laboratory study of borehole breakouts in Cordova Cream: a case of shear failure mechanism. Int. J. Rock Mech. Min. Sci. Geomech. Abstr. 30 (7), 1047–1056.

Halchuk, S., Mereu, R., 1990. A seismic investigation of the crust and Moho underlying the Peace River Arch, Canada. Tectonophysics 185 (1–2), 1–19.

Hamid, O., 2008. In-situ stress analysis of Southwest Saskatchewan. (Master thesis) University of Saskatchewan, Saskatchewan.

Hancock, P.L., 1991. Determining contemporary stress directions from neotectonic joint systems [and discussion]. Philos. Trans. R. Soc. A Math. Phys. Eng. Sci. 337 (1645), 29–40.

Hancock, P.L., Engelder, T., 1989. Neotectonic joints. Geol. Soc. Am. Bull. 101 (10), 1197–1208.

Hansen, K.M., Mount, V.S., 1990. Smoothing and extrapolation of crustal stress orientation measurements. J. Geophys. Res. 95 (B2), 1155–1165.

Heidbach, O., Ben-Avraham, Z., 2007. Stress evolution and seismic hazard of the Dead Sea Fault System. Earth Planet. Sci. Lett. 257 (1–2), 299–312.

Heidbach, O., Reinecker, J., Tingay, M.R., Müller, B., Sperner, B., Fuchs, K., Wenzel, F., 2007. Plate boundary forces are not enough: second- and third-order stress patterns highlighted in the World Stress Map database. Tectonics 26 (6), 1–19.

Heidbach, O., Tingay, M. R., Barth, A., Reinecker, J., Kurfeß, D., Müller, B., 2009. The World Stress Map based on the database release 2008, equatorial scale 1:46,000,000. Technical Report 3, Commission for the Geological Map of the World, Paris.

Heidbach, O., Tingay, M.R.P., Barth, A., Reinecker, J., Kurfeß, D., Müller, B., 2010. Global crustal stress pattern based on the World Stress Map database release 2008. Tectonophysics 482 (1–4), 3–15.

Henton, J.A., Craymer, M.R., Ferland, R., Dragert, H., Mazzotti, S., Forbes, D.L., 2006. Crustal motion and deformation monitoring of the Canadian landmass. Geomatica 60 (2), 173–191.

Hodges, J.L., Lehmann, E.L., 1967. On medians and quasi medians. J. Am. Stat. Assoc. 62 (319), 926–931.

Hoffman, P.F., 1989. Precambrian geology and tectonic history of North America. The Geology of North America. The Geological Society of America, pp. 447–512.

Hottman, C., Smith, J., Purcell, W., 1979. Relationship among earth stresses, pore pressure, and drilling problems offshore Gulf of Alaska. J. Pet. Technol. 31 (11).

Huang, J., Véronneau, M., 2005. Applications of downward-continuation in gravimetric geoid modeling: case studies in Western Canada. J. Geod. 79 (1–3), 135–145.

Hubbert, M.K., Willis, D.G., 1957. Mechanics of hydraulic fracturing. AIME Trans 210, 153–168.

Humphreys, E.D., Coblentz, D.D., 2007. North American dynamics and western U.S. tectonics. Rev. Geophys. 45 (3), 30.

Hurd, O., Zoback, M.D., 2012. Intraplate earthquakes, regional stress and fault mechanics in the Central and Eastern U.S. and Southeastern Canada. Tectonophysics 581, 182–192.

Kao, H., Behr, Y., Currie, C.A., Hyndman, R.D., Townend, J., Lin, F.-C., Ritzwoller, M.H., Shan, S.-J., He, J., 2013. Ambient seismic noise tomography of Canada and adjacent regions: part I. Crustal structures. J. Geophys. Res. Solid Earth 118 (11), 5865–5887.

Kim, W.-Y., 2003. The 18 June 2002 Caborn, Indiana, Earthquake: reactivation of ancient rift in the Wabash Valley Seismic Zone? Bull. Seismol. Soc. Am. 93 (5), 2201–2211.

Kim, W.-Y., Dineva, S., Ma, S., Eaton, D.W., 2006. The 4 August 2004, Lake Ontario, Earthquake. Seismol. Res. Lett. 77 (1), 65–73.

Kirby, J.F., Swain, C.J., 2014. The long wavelength admittance and effective elastic thickness of the Canadian shield. J. Geophys. Res. Solid Earth 119, 28.

Konstantinovskaya, E., Malo, M., Castillo, D., 2012. Present-day stress analysis of the St. Lawrence Lowlands sedimentary basin (Canada) and implications for caprock integrity during CO_2 injection operations. Tectonophysics 518–521, 119–137.

Li, Y.G., Leary, P.C., Henyey, T.L., 1988. Stress orientation inferred from shear wave splitting in basement rock at Cajon Pass. Geophys. Res. Lett. 15 (9), 997–1000.

Ljunggren, C., Chang, Y., Janson, T., Christiansson, R., 2003. An overview of rock stress measurement methods. Int. J. Rock Mech. Min. Sci. 40 (7–8), 975–989.

Ma, S., Eaton, D.W., Adams, J.J., 2008. Intraplate seismicity of a recently deglaciated shield terrane: a case study from Northern Ontario, Canada. Bull. Seismol. Soc. Am. 98 (6), 2828–2848.

Mardia, K., 1972. Statistics of Directional Data. Academic Press, London and New York.

Mazzotti, S., Hyndman, R.D., 2002. Yakutat collision and strain transfer across the northern Canadian Cordillera. Geology 30 (6), 495.

Mazzotti, S., Townend, J., 2010. State of stress in central and eastern North American seismic zones. Lithosphere 2 (2), 76–83.

McGarr, A., 1982. Analysis of states of stress between provinces of constant stress. J. Geophys. Res. 87 (B11), 9279.

McGarr, A., Gay, N.C., 1978. State of stress in the earth's crust. Annu. Rev. Earth Planet. Sci. 6, 405–436.

McKenzie, D., 1969. The relation between fault plane solutions for earthquakes and the directions of the principal stresses. Bull. Seismol. Soc. Am. 2, 591–601.

McMechan, M.E., Price, R.A., 1982. Transverse folding and superposed deformation, Mount Fisher area, southern Canadian Rocky Mountain thrust and fold belt. Can. J. Earth Sci. 19 (5), 1011–1024.

Michael, A.J., 1987. Use of focal mechanisms to determine stress: a control study. J. Geophys. Res. 92 (B1), 357–368.

Michael, K., Buschkuehle, M., 2008. Subsurface characterization of acid-gas injection operations in the Peace River Arch Area. Energy Resources Conservation Board, ERCB/AGS Special Report 090,pp. 1–186.

Monger, J., Price, R.A., 2002. The Canadian Cordillera: geology and tectonic evolution. CSEG Rec. 27, 17–36.

Monger, J., Souther, J., Gabrielse, H., 1972. Evolution of the Canadian Cordillera; a plate-tectonic model. Am. J. Sci. 272 (7), 577–602.

Mossop, G.D., Shetsen, I. (Eds.), 1994. Geological Atlas of the Western Canada Sedimentary Basin. Canadian Society of Petroleum Geologists and Alberta Research Council.

Müller, B., Wehrle, V., Zeyen, H., Fuchs, K., 1997. Short-scale variations of tectonic regimes in the western European stress province north of the Alps and Pyrenees. Tectonophysics 275 (1–3), 199–219.

Müller, B., Wehrle, V., Hettel, S., Sperner, B., Fuchs, K., 2003. A new method for smoothing orientated data and its application to stress data. Geol. Soc. Lond., Spec. Publ. 209 (1), 107–126.

Nakamura, K., 1977. Volcanoes as possible indicators of tectonic stress orientation principle and proposal. J. Volcanol. Geotherm. Res. 2 (1), 1–16.

Nakamura, K., Jacob, K.H., Davies, J.N., 1977. Volcanoes as possible indicators of tectonic stress orientation Aleutians and Alaska. Pure Appl. Geophys. 115 (1–2), 87–112.

Naliboff, J., Lithgow-Bertelloni, C., Ruff, L., de Koker, N., 2012. The effects of lithospheric thickness and density structure on Earth's stress field. Geophys. J. Int. 188 (1), 1–17.

Norris, A., 1986. Review of Hudson platform paleozoic stratigraphy and biostratigraphy. In: Martini, I.P. (Ed.), Canadian Inland Seas. Elsevier Science Publishing Company Inc., pp. 494–503.

NRCan (2009). Atlas of Canada 6th Edition — Geological Provinces.

Oakey, G.N., Stephenson, R., 2008. Crustal structure of the Innuitian region of Arctic Canada and Greenland from gravity modelling: implications for the Palaeogene Eurekan orogen. Geophys. J. Int. 173 (3), 1039–1063.

Obert, L., 1962. In situ determination of stress in rock. Min. Eng. 14, 51–58.

Plumb, R.A., Hickman, S.H., 1985. Stress-induced borehole elongation: a comparison between the four-arm dipmeter and the borehole televiewer in the Auburn Geothermal Well. J. Geophys. Res. 90 (B7), 5513–5521.

Pollock, J.C., Hibbard, J.P., Staal, C.R.V., 2012. A paleogeographical review of the peri-Gondwanan realm of the Appalachian orogen. Can. J. Earth Sci. 288 (1), 259–288.

Porter, J.W., Price, R.A., McCrossan, R.G., 1982. The Western Canada Sedimentary Basin. Philos. Trans. R. Soc. Lond. 305 (1489), 169–192.

Price, R., 1981a. The Cordilleran foreland thrust and fold belt in the southern Canadian Rocky Mountains. In: McClay, K.R., Price, R.A. (Eds.), Thrust and Nappe Tectonics. The Geological Society of London, pp. 427–448.

Price, R.A., 1981b. The Cordilleran foreland thrust and fold belt in the southern Canadian Rocky Mountains. Geol. Soc. Lond., Spec. Publ. 9 (1), 427–448.

Price, R.A., 1986. The southeastern Canadian Cordillera: thrust faulting, tectonic wedging, and delamination of the lithosphere. J. Struct. Geol. 8 (3–4), 239–254.

Price, R.A., 1994. Cordilleran tectonics and the evolution of the Western Canada Sedimentary Basin. In: Mossop, G.D., Shetsen, I. (Eds.), Geological Atlas of the Western Canada Sedimentary Basin. Canadian Society of Petroleum Geologists and Alberta Research Council, pp. 13–24 (chapter 2).

Raleigh, C.B., Healy, J.H., Bredehoeft, J.D., 1972. Faulting and crustal stress at Rangely, Colorado. In: Heard, H.C., Borg, I.Y., Carter, N.L., Raleigh, C.B. (Eds.), Flow and Fracture of Rocks. vol. 16. U.S. Geological Survey, pp. 275–284.

Ratanaruamkarn, S., Niewiadomska-Bugaj, M., Wang, J.-C., 2009. A new estimator of a circular median. Commun. Stat. Simul. Comput. 38 (6), 1269–1291.

Rebaï, S., Philip, H., Taboada, A., 1992. Modern tectonic stress field in the Mediterranean region: evidence for variation in stress directions at different scales. Geophys. J. Int. 110 (1), 106–140.

Reinecker, J., Tingay, M.R., Müller, B., 2003. Borehole breakout analysis from four-arm caliper logs. Technical ReportWorld Stress Map Project.

Reinecker, J., Tingay, M., Müller, B., Heidbach, O., 2010. Present-day stress orientation in the Molasse Basin. Tectonophysics 482 (1–4), 129–138.

Please cite this article as: Reiter, K., et al., A revised crustal stress orientation database for Canada, Tectonophysics (2014), http://dx.doi.org/10.1016/j.tecto.2014.08.006

Reiter, K., Heidbach, O., 2014. Calibration of a 3D–geomechanical–numerical model of the contemporary crustal stress state in the Alberta Basin. Solid Earth Discuss. 6, 2423–2494. http://dx.doi.org/10.5194/sed-6-2423-2014.
Richardson, R.M., 1992. Ridge forces, absolute plate motions, and the intraplate stress field. J. Geophys. Res. 97 (B8), 11739–11748.
Richardson, R.M., Reding, L.M., 1991. North American plate dynamics. J. Geophys. Res. 96 (B7), 12201–12223.
Ristau, J., Rogers, G.C., Cassidy, J.F., 2007. Stress in western Canada from regional moment tensor analysis. Can. J. Earth Sci. 44 (2), 127–148.
Ruppert, N.A., 2008. Stress map for Alaska from earthquake focal mechanisms. Geophys. Monogr. 179, 351–367.
Sbar, M.L., Sykes, L.R., 1973. Contemporary compressive stress and seismicity in eastern North America: an example of intra-plate tectonics. Geol. Soc. Am. Bull. 84 (6), 1861–1882.
Schmitt, D.R., Currie, C.A., Zhang, L., 2012. Crustal stress determination from boreholes and rock cores: fundamental principles. Tectonophysics 580, 1–26.
Sigloch, K., Mihalynuk, M.G., 2013. Intra-oceanic subduction shaped the assembly of Cordilleran North America. Nature 496 (7443), 50–56.
Sperner, B., Müller, B., Heidbach, O., Delvaux, D., Reinecker, J., Fuchs, K., 2003. Tectonic stress in the Earth's crust: advances in the World Stress Map project. Geochem. Soc. Spec. Publ. 212, 101–116.
Steffen, R., Eaton, D.W., Wu, P., 2012. Moment tensors, state of stress and their relation to post-glacial rebound in northeastern Canada. Geophys. J. Int. 189 (3), 1741–1752.
StLouisEQcenter, 2010. St. Louis University Earthquake Center.
Tingay, M.R.P., Müller, B., Reinecker, J., Heidbach, O., Wenzel, F., Fleckenstein, P., 2005. Understanding tectonic stress in the oil patch: the World Stress Map project. Lead. Edge 24 (12), 1276–1282.
Tingay, M.R., Reinecker, J., Müller, B., 2008. Borehole breakout and drilling-induced fracture analysis from image logs. Technical ReportWorld Stress Map Project.
Upton, G., Cook, I.T., 1996. Understanding Statistics. Oxford University Press.
Véronneau, M., 1997. The GSD95 geoid model for Canada. Technical ReportGeodetic Survey Division, Dept. of Natural Resources, Ottawa.
Wahlstrom, R., 1987. The North Gower, Ontario, earthquake of 11 October 1983: focal mechanism and aftershocks. Seismol. Res. Lett. 58 (3), 65–72.
Wessel, P., Smith, W.H.F., Scharroo, R., Luis, J., Wobbe, F., 2013. Generic mapping tools: improved version released. EOS Trans. Am. Geophys. Union 94 (45), 409–410.
White, A.J., Traugott, M.O., Swarbrick, R.E., 2002. The use of leak-off tests as means of predicting minimum in-situ stress. Pet. Geosci. 8 (2), 189–193.
Wright, G., McMechan, M., Potter, D., 1994. Structure and architecture of the Western Canada Sedimentary Basin. In: Mossop, G.D., Shetsen, I. (Eds.), Geological Atlas of the Western Canada Sedimentary Basin. Canadian Society of Petroleum Geologists and Alberta Research Council, pp. 25–40 (chapter 3).
Yassir, N.A., Bell, J.S., 1994. Relationships between pore pressure, stresses, and present-day geodynamics in the Scotian Shelf, offshore eastern Canada. AAPG Bull. 78 (12), 1863–1880.
Yassir, N.A., Dusseault, M.B., 1992. Stress trajectory determinations in southwestern Ontario from borehole logs. Geol. Soc. Lond., Spec. Publ. 65 (1), 169–177.
Zakharova, N.V., Goldberg, D.S., 2014. In situ stress analysis in the northern Newark Basin: implications for induced seismicity from CO_2 injection. J. Geophys. Res. Solid Earth 119 (3), 2362–2374.
Zang, A., Stephansson, O., 2010. Stress Field of the Earth's Crust. Springer, Netherlands, Dordrecht.
Zemanek, J., Caldwell, R., Glenn, E.E., Holcomb, S., Norton, L., Straus, A., 1969. The borehole televiewer—a new logging concept for fracture location and other types of borehole inspection. J. Pet. Technol. 21 (6).
Zemanek, J., Glenn, E.E., Norton, L.J., Caldwell, R.L., 1970. Formation evaluation by inspection with the borehole televiewer. Geophysics 35 (2), 254–269.
Zoback, M.L., 1992. First- and second-order patterns of stress in the lithosphere: the World Stress Map project. J. Geophys. Res. 97 (B8), 11703–11728.
Zoback, M.L., Mooney, W.D., 2003. Lithospheric buoyancy and continental intraplate stresses. Int. Geol. Rev. 45 (2), 95–118.
Zoback, M.L., Zoback, M.D., 1980. State of stress in the conterminous United States. J. Geophys. Res. 85 (B11), 6113–6156.
Zoback, M.D., Zoback, M.L., 1981. State of stress and intraplate earthquakes in the United States. Science (New York, N.Y.) 213 (4503), 96–104.
Zoback, M.L., Zoback, M.D., 1989. Tectonic stress field of the continental United States, In: Pakiser, L., Mooney, W.D. (Eds.), Geophysical Framework of the Continental United States, Geological edition vol. 172. Geological Society of America, pp. 523–540 chapter 24.
Zoback, M.D., Zoback, M.L., 1991. Tectonic stress field of North America and relative plate motions. In: Slemmons, D.B., Engdahl, E.R. (Eds.), Neotectonics of North America. Geological Society of America, pp. 339–366.
Zoback, M.D., Moos, D., Mastin, L., Anderson, R.N., 1985. Well bore breakouts and in situ stress. J. Geophys. Res. 90 (B7), 5523–5530.
Zoback, M.L., Zoback, M.D., Adams, J.J., Assumpção, M., Bell, J.S., Bergman, E.A., Blümling, P., Brereton, N.R., Denham, D., Ding, J., Fuchs, K., Gay, N., Gregersen, S., Gupta, H.K., Gvishiani, A., Jacob, K., Klein, R., Knoll, P., Magee, M., Mercier, J.L., Müller, B.C., Paquin, C., Rajendran, K., Stephansson, O., Suarez, G., Suter, M., Udias, A., Xu, Z.H., Zhizhin, M., 1989. Global patterns of tectonic stress. Nature 341 (6240), 291–298.
Zoback, M.D., Barton, C.A., Brudy, M., Castillo, D.A., Finkbeiner, T., Grollimund, B.R., Moos, D.B., Peska, P., Ward, C.D., Wiprut, D.J., 2003. Determination of stress orientation and magnitude in deep wells. Int. J. Rock Mech. Min. Sci. 40 (7–8), 1049–1076.

Please cite this article as: Reiter, K., et al., A revised crustal stress orientation database for Canada, Tectonophysics (2014), http://dx.doi.org/10.1016/j.tecto.2014.08.006